Review of Scientific Instruments

Ion temperature measurement techniques using fast sweeping retarding field analyzer (RFA) in strongly intermittent ASDEX Upgrade tokamak plasmas

R. Ochoukov[1,*], M. Dreval[2], V. Bobkov[1], H. Faugel[1], A. Herrmann[1], L. Kammerloher[1], P. Leitenstern[1], ASDEX Upgrade Team[a)], and EUROfusion MST1 Team[b)]

[1]Max Planck Institute for Plasma Physics, Boltzmannstr. 2, 85748 Garching, Germany
[2]Institute of Plasma Physics, National Science Center 'Kharkov Institute of Physics and Technology', Kharkov 61108, Ukraine

*corresponding author email: rochouko@ipp.mpg.de

Abstract

The manuscript presents a new method of interpreting the ion temperature (T_i) measurement with a retarding field analyzer (RFA) that accounts for the intermittent/turbulent nature of the scrape off layer (SOL) plasmas in tokamaks. Fast measurements and statistical methods are desirable for an adequate description of random fluctuations caused by such intermittent events as edge localized modes (ELMs) and blobs. We use an RFA that can sweep its current-voltage (I-V) characteristics with up to 10 kHz. The RFA uses an electronics compensation stage to subtract the capacitive pick-up due to the finite connecting cable capacitance, which greatly improves the signal-to-noise ratio. In the 10 kHz case, a single I-V characteristic is obtained in time that is an order of magnitude faster than the ELM cycle. The fast sweeping frequency allows us to reconstruct the T_i probability density function (PDF), which we use as the T_i representation. The boundary conditions that we place on the I-V characteristics when calculating the T_i values impact the resulting T_i PDF. If the boundaries are insensitive to the plasma fluctuations then the most probable T_i value of the PDF (20-25 eV) is similar to the T_i value obtained via the classical conditional averaging method (20-27 eV). However, if the boundary conditions follow the fluctuations then the PDF-based method gives a substantially higher most probable T_i value (35-60 eV). Overall, we show that a fast sweeping RFA diagnostic should be used in intermittent SOL plasmas to reconstruct the probability density function for accurate T_i measurements.

1. Introduction

The character of scrape off layer (SOL) plasma in modern tokamaks is strongly intermittent [1]. Edge localized modes (ELMs) in H-mode plasmas can cause significant plasma density and temperature perturbations in the SOL region [2]. Blobs are usually present at the plasma edge and also cause substantial jumps of the SOL parameters over time [3-7]. The time scale up to or greater than 1 ms is typical for the SOL plasma intermittence. Such plasma behavior causes abrupt changes of raw SOL diagnostics signals. Temporal resolution of the SOL diagnostics should be substantially higher than the typical rate of the plasma intermittence to resolve the turbulence for accurate measurements. This resolution in some SOL diagnostics, like classical single-pin Langmuir probes [8], is restricted by how quickly the applied voltage is swept. Fast enough sweeping of at least 10 kHz is required for accurate measurements. Such fast sweeping frequency presents a set of technical difficulties of the diagnostic electronics design. Substantial diagnostic cable capacitance can distort measured signals and sweeping voltage values at the diagnostic electrodes due to the integration effect. The capacitive pick-up current between diagnostic cables is strongly rising with the sweeping frequency too. However, Langmuir probe techniques with extremely fast applied voltage sweeps are developed [9, 10]. The voltage-sweeping techniques are usually avoided in most of the SOL diagnostics by an improvement of the diagnostic principal, for example by using a triple probe [11] or a ball-pen probe technique [12]. In the retarding field analyzer (RFA) diagnostic, the classical voltage-sweeping technique [13-17] can be applied at a fast (10 kHz) rate [18] or, alternatively, be replaced by a DC

a) see the author list in H. Meyer et al. 2019 Nucl. Fusion 59 112014.
b) see the author list in B. Labit et al. 2019 Nucl. Fusion 59 086020.

operation [19, 20]. However, the 3-grid RFA design and the proper selection of two repelling voltages complicates the DC operation technique implementation. The RFA in classical voltage-sweeping technique provides ion temperature (T_i) and energy distribution data in the SOL region. Although strong capacitive coupling between connecting cables from the RFA grid and the RFA collector causes strong interference even at the sweeping frequency of 0.5-1 kHz. As a result, special designs of the diagnostic electronics are used for the suppression of this interference [14, 15]. Our novel design of RFA electronics and 10 kHz sweeping technique realization in the ASDEX-U tokamak is described in this work.

A classical approach to the intermittent RFA data analysis is based on the measurement of conditionally averaged plasma parameters [14-17]. In this case the measurement time is significantly longer than the time of plasma intermittence and the fluctuations are averaged numerically. This approach is frequently used in tokamaks. However, this approach can cause substantial errors in the ion temperature measurement by the RFA, as it is shown in our work. The influence of plasma fluctuations on the RFA measurements is considered only in a few recent works [19, 20] using the DC RFA operation technique. We are considering a different approach based on the fast sweeping technique. In the case of intermittent probes data analysis statistical moments of distribution functions are used for the probabilistic data description [6, 7]. We choose to follow the probabilistic approach when estimating the ion temperature via a fast sweeping RFA diagnostic: the ion temperature is represented by the most probable value of the T_i probability density function (PDF). We also show that the PDF-based T_i values depend on the boundary conditions used when reconstructing the PDF. If the boundary conditions are such that they ignore plasma fluctuations, then the resulting most probable T_i matches the T_i value from the conditional averaging method. However, when the boundary conditions follow fluctuations, then the most probable T_i is substantially higher.

2. Experimental setup

All the measurements described in this manuscript were performed in ASDEX Upgrade: a medium sized diverted tokamak (Fig. 1 (a)). The plasma discharges were performed in helium and the target

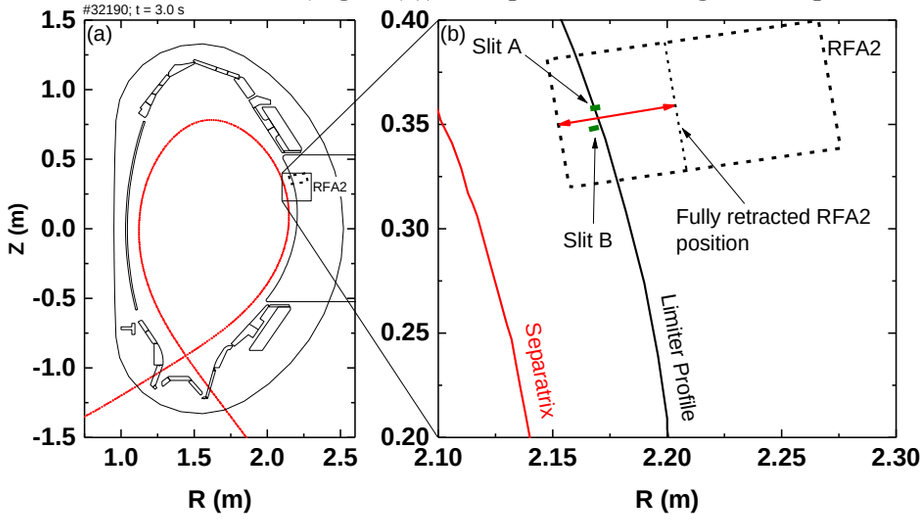

Figure 1: A detailed poloidal cross sectional view of the ASDEX Upgrade in-vessel structures, with the RFA2 position highlighted. (a) A large scale view of the entire vessel and (b) a detailed view of the region where RFA2 is installed. The red double-sided arrow in (b) shows the radial extent of the RFA2 movement.

discharge was an H-mode, maintained via constant 3.7 MW of electron cyclotron resonant heating (ECRH) and 5.4 MW of neutral beam injected (NBI) power. The on-axis magnetic field was -2.5 T (negative sign implied counter current direction) and the plasma current was 0.8 MA. The ion temperature in the SOL was measured with a retracting RFA (hereby referred as RFA2, to differentiate from the originally installed RFA diagnostic on the midplane manipulator [16]), that sits ~0.35 m above the midplane (Fig. 1 (b)). The SOL plasma is sampled by the RFA2 diagnostic when it is fully radially inserted towards the plasma (Fig. 1 (b)). RFA2 consists of two independent analyzers, sampling the plasma flux tubes parallel (Side B) and antiparallel (Side A) to the background magnetic field (Fig. 2). A detailed description of the analyzer is provided in [14, 15], we only briefly

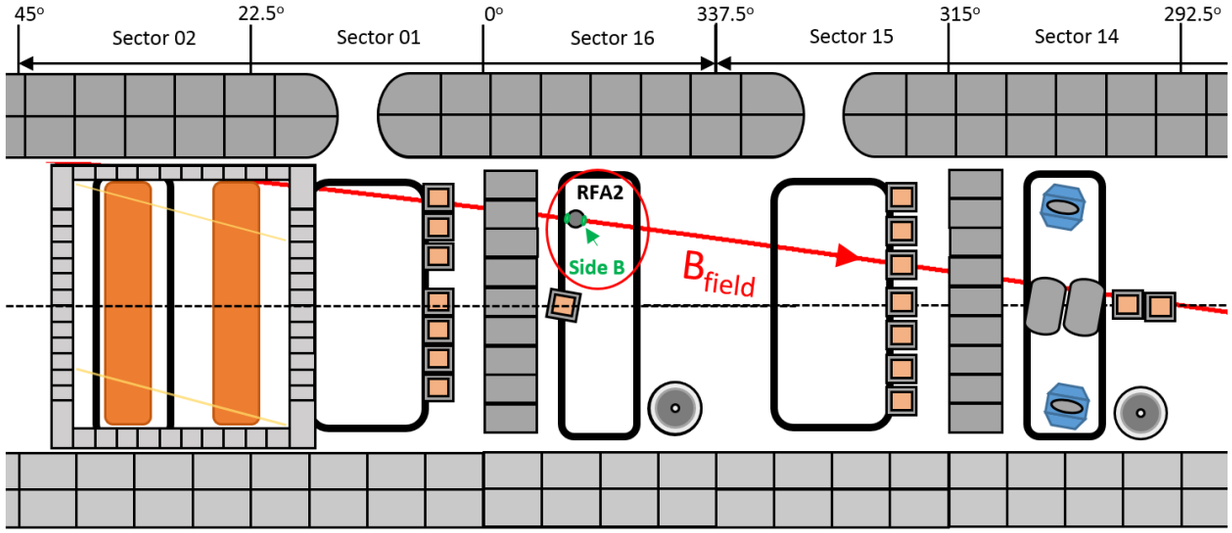

Figure 2: An unfolded view of the ASDEX Upgrade outer wall. RFA2 is installed in Sector 16, ~35 cm above the midplane (the midplane position is indicated by a horizontal dashed line). The RFA2 toroidal orientation is tilted by ~10° to match the orientation of the local magnetic field line. Side B of RFA2, which samples the plasma flux tube from the midplane, is indicated.

summarize the relevant key principles of operation in here, refer to Fig. 2 in [13]. We use the slit plate voltage V_{slit} = -100 V to repel the plasma electron fraction from entering the analyzer. The remaining ions then pass through a pair of biased grids, the purpose of the first grid (Grid 1) is to periodically sweep the voltage (V_{gr1}) positively enough to fully interrogate the ion kinetic energy distribution function (and hence extract the bulk T_i profile). The second grid (Grid 2) is biased negatively (V_{gr2} = -150 V in our case) and constant to help mitigate a secondary electron current that may arise due to the ions striking the collector surface. The final component is the grounded collector that measures the impinging ion current (I_{coll}). The ion collection current is defined as "positive" in the presented data. All the potentials are referenced with respect to the grounded vessel.

3. Modification of the RFA diagnostics for the fast sweeping technique implementation

In order to achieve our goal of measuring RFA I-V characteristics fast enough to fully resolve turbulent filaments and ELMs we use an FLC Electronics fast sweeping bipolar amplifier model A800D (voltage sweeping frequency f_s up to 100 kHz while maintaining peak-to-peak current (I_{PP}) and voltage (V_{PP}) values up to 60 mA and 800 V, respectively [21]). All voltage and current signals are digitized at 2 MHz via an ASDEX Upgrade-developed serial input-output-based (or SIO-based) data acquisition system [22]. As the frequency sweep of the grid 1 bias voltage is increased, the capacitive pickup currents (primarily due to the finite connecting cable capacitance) eventually begin to dominate over the ion currents due to plasma. The nominal capacitive currents I_c at f_s = 1 kHz are ~1-2 μA, about 1 order of magnitude lower than the typical ion saturation current due to plasma. However, for f_s > 10 kHz, I_c becomes comparable or even larger than the ion current from plasma as I_c scales linearly with dV_{grl}/dt and f_s. To remove this parasitic capacitive current from the measured I_{coll} values, we use a differential operational amplifier (op-amp) where the probe signal is applied to the positive op-amp input and a "mirror" capacitance c_{mirror} is applied to the negative op-amp input (Fig. 3). The resulting op-amp output is V_{out} ~$(c_{probe} - c_{mirror})dV_{grl}/dt$. As long as the mirror

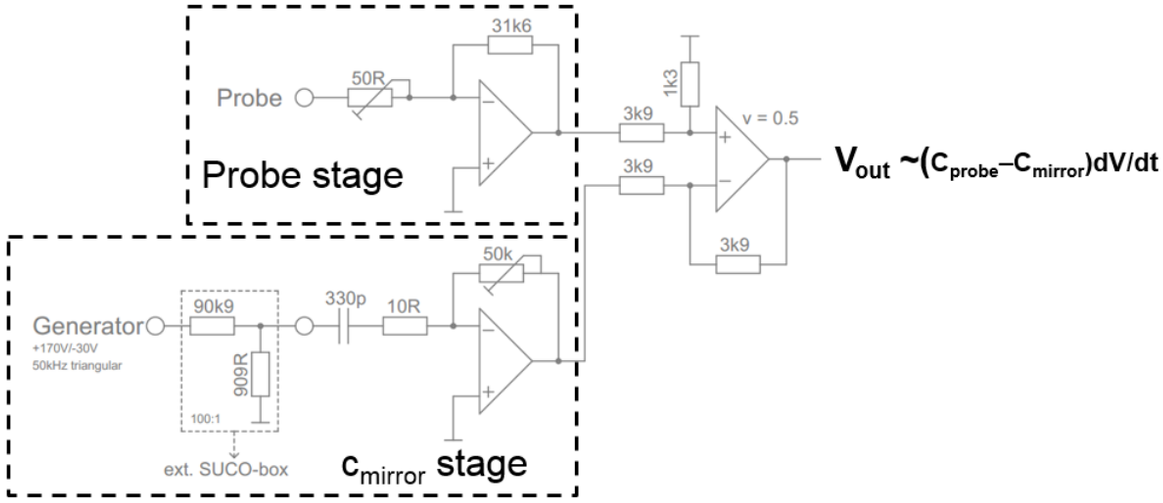

Figure 3: An electrical circuit diagram for the components used to remove the capacitive pick-up current due to the finite cable capacitance.

capacitance is well matched to the probe cable capacitance (in vacuum, without plasma) V_{out} remains independent of dV_{gr1}/dt and f_s (Figs. 4 (a), (c) and (e), Side B curves). Note that in the vicinity of the points where the grid 1 voltage reaches its maximum or minimum values and reverses its sweep direction, we have a finite d^2V/dt^2 term (which is otherwise equal to zero for a triangular waveform).

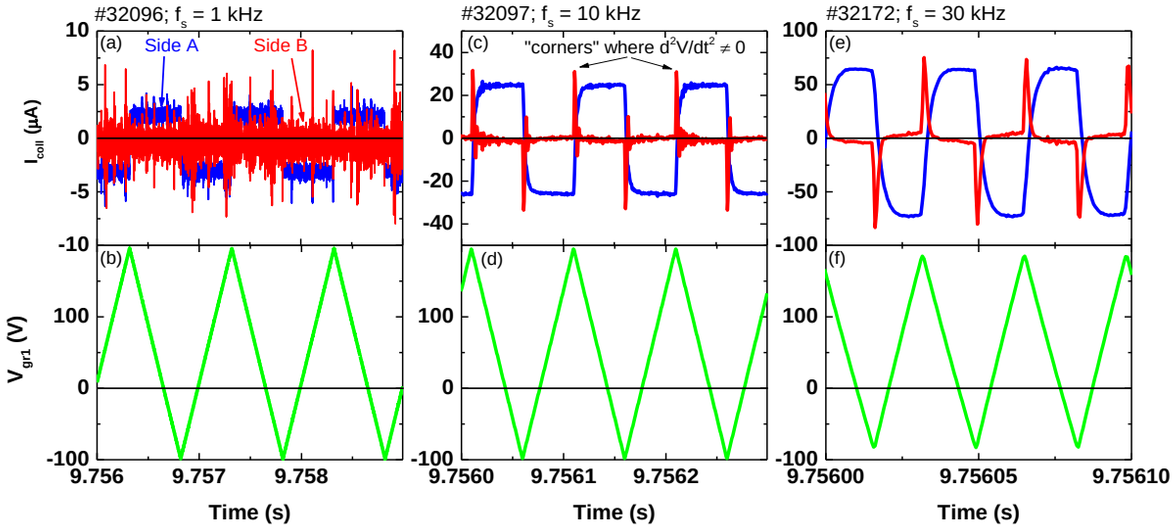

Figure 4: Raw (Side A) and capacitively compensated (Side B) collector current (I_{coll}) examples at three different sweep frequencies (f_s) of the grid 1 bias voltage (V_{gr1}). (a), (c), and (e) are the collector current values at f_s = 1 kHz, 10 kHz, and 30 kHz, respectively. (b), (d), and (f) are the grid 1 bias voltages (V_{gr1}) at the three sweep frequencies. Note the different Y-axis scales for (a), (c), and (e).

This inductive response of the electronics causes the appearance of I_{coll} "corners" clearly visible in Figs. 4 (c) and (e). These "corners" are avoided by using a sinusoidal V_{gr1} waveform, as will be shown in the next section of the manuscript.

4. Comparison of the various RFA techniques

4.1. Techniques for RFA ion temperature estimation via conditional averaging

First let us start the comparison with a classical RFA analysis method based on conditional averaging. We use a slow sweeping frequency of 100 Hz, with a sinusoidal grid 1 voltage waveform ranging from -50 to 110 V. Raw RFA V_{gr1} and I_{coll} data from ASDEX Upgrade discharge #36676 is shown in Fig. 5. The RFA position is fixed in this discharge at the fully inserted orientation (Fig. 1 (b)).

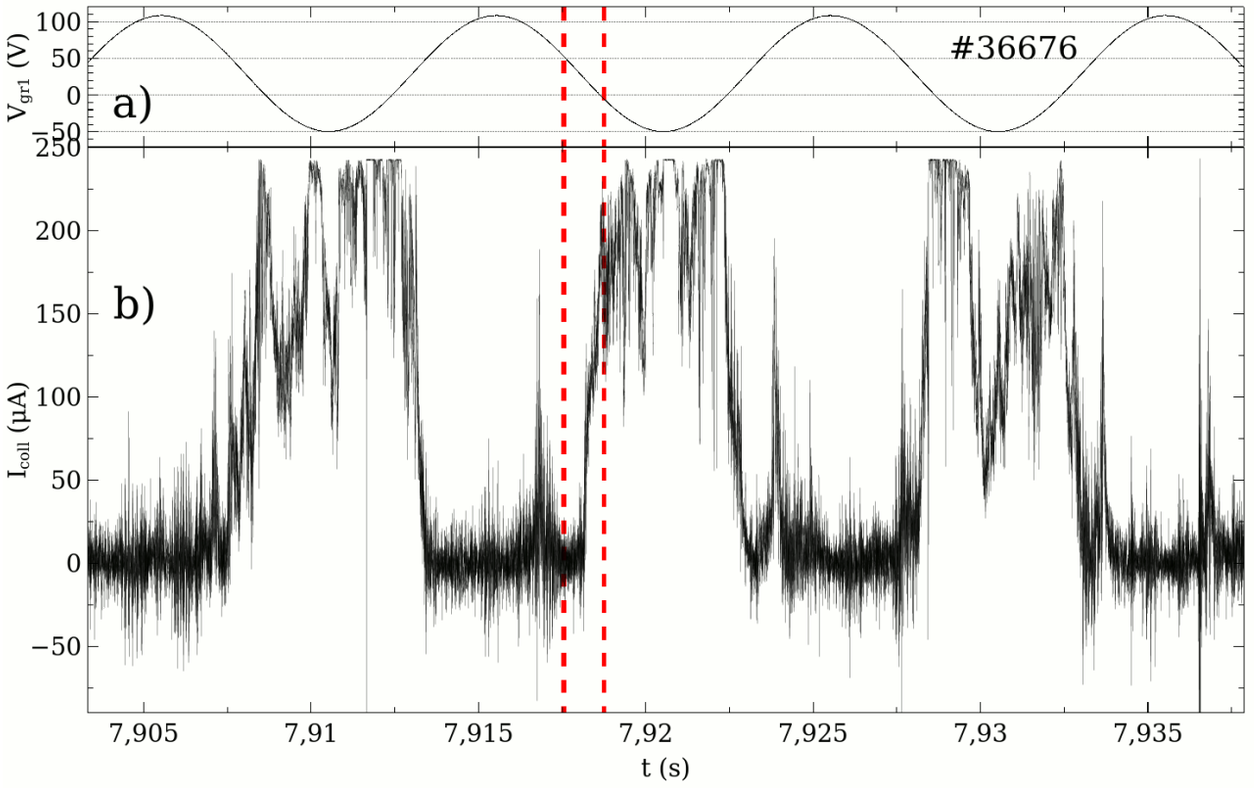

Figure 5: (a) The RFA grid 1 voltage (V_{gr1}) and (b) the collector current (I_{coll}) in discharge #36676 for RFA2 Side A. The sweep frequency f_s is 100 Hz. The RFA2 position is fixed. The vertical dashed lines indicate the I-V region used in data analysis.

Raw I_{coll} data (Fig. 5 (b)) demonstrates the intermittent character of the signal, determined by H-mode confinement with ELMs in this discharge. Three sweeping voltage stages are clearly seen in Fig. 5. At the stages of high sweeping voltage ($V_{gr1} > 50$ V) no pronounced ion current is observed. The signal at these stages is dominated by electronics noise. The noise character is not symmetric, as it is seen from these stages. At the stages with low enough sweeping voltages ($V_{gr1} < 0$) all ions are passing to the RFA collector. The signal fluctuations at these stages are determined by fluctuations of the plasma density, the ion temperature, and the plasma potential at the RFA position. The voltage value about 0 V corresponds to the plasma potential and defines the so-called knee potential (V_{knee}) of the I-V curve (Fig. 6). At the intermediate voltage stages 5-50 V a clear I-V characteristic slope is observed due to fractional repelling of the ion distribution function by the sweeping grid 1 voltage. The RFA collector current of Fig. 5 (b) is plotted versus the swept grid 1 voltage in Fig. 6.

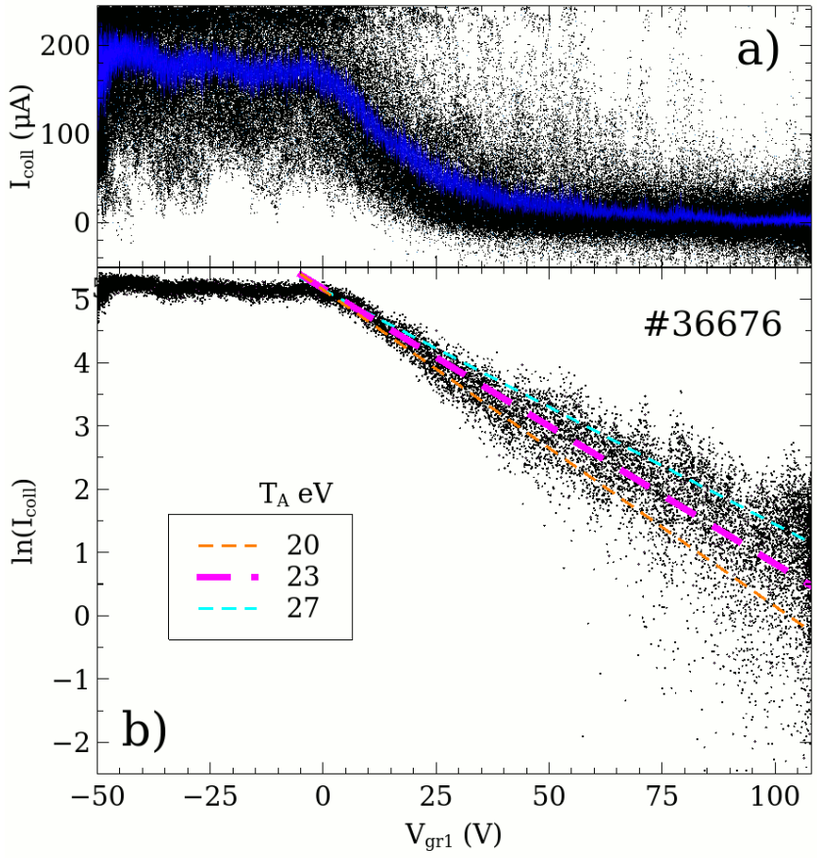

Figure 6: The RFA2 I-V curve in discharge #36676. Data from a 30 ms time window is plotted on (a) a linear and (b) a logarithmic scale. Raw data in (a) is shown by black dots and conditionally averaged data is shown by blue lines. The Side A analyzer is used. The estimated T_i value is 23 eV, or 20-27 eV within the error bars.

We are now considering a simple conditional average (or mean) of the RFA collector current signal versus time, which is a most frequently used method for RFA data interpretation. Raw I_{coll} data from 3 consecutive periods of V_{gr1} (a 30 ms time interval) is plotted versus V_{gr1} using black dots in Fig. 6 (a). We apply numerical averaging to I_{coll} data versus V_{gr1}, shown by the blue line in Fig. 6 (a). After removing negative I_{coll} data points, we take the natural logarithm from this averaged signal, as shown in Fig. 6 (b). The V_{knee} value is clearly observed in Fig. 6. The logarithmic I-V slope is well described by a linear fit corresponding to a single ion temperature of 23 eV (within the error bar window of 20-27 eV). We assume singly charged He ion species when estimating the ion temperature from the I-V slopes. The raw RFA collector current signal is very intermittent, as it is seen from Fig. 5. This noise-like character is well-correlated to the ELMs. A typical rate of the plasma intermittence caused by the ELMs is represented by the divertor D_α diagnostic (Fig. 7).

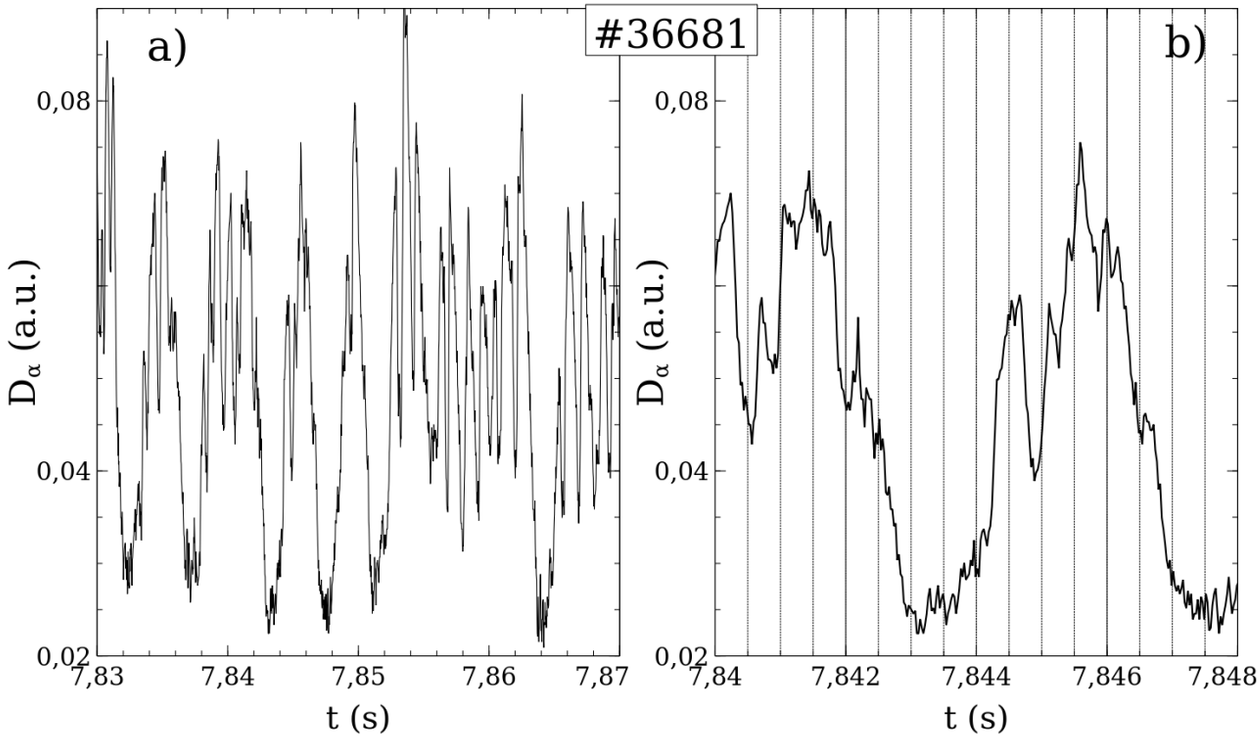

Figure 7: ELMs observed by the divertor D_α diagnostic in two time windows in discharge #36681, which is nearly identical to #36676. (a) A long (or slow) time window and (b) a short (or fast) time window.

The typical ELM cycle rate is ~0.5 ms, as it is shown in Fig. 7. The 10 kHz sweeping rate allows us to measure RFA I-V's every 0.05 ms, which corresponds to 1/2 of the sweeping period. As a result, the 10 kHz sweeping rate is fast enough for the ELMy H-mode plasma under consideration. Raw and processed data of 10 kHz RFA sweeps in ASDEX Upgrade discharge #36681 is shown in Fig 8. The discharges #36676 and #36681 have nearly identical plasma parameters and, hence, can be used for comparison. The intermittent character of the RFA I_{coll} signal is more apparent in the 10 kHz sweeping case (Fig. 8 (b)). The plasma density drops seen in the 100 Hz case, for example, at 7.93 s (Fig. 5 (b)), lower the amplitude of the entire I-V curve in the 10 kHz case , for example at 7.873 s (Fig. 8 (b)). The time evolution of the ion temperature calculated using the data from two neighboring slopes is shown in Fig. 8 (c). Two fitting criteria of the temperature calculation are used as indicated in the legend. These criteria will be discussed in the proceeding sections of the manuscript.

To stay consistent with the fitting routine applied at 100 Hz (Fig. 6), we apply the same data analysis implementation to the 10 kHz case. The RFA I-V data over a 30 ms time window is plotted in Fig. 9. Comparison of Figs. 6 and 9 data shows quite similar results for 100 Hz and 10 kHz sweeping cases. Similar I-V slopes are observed, but in the 10 kHz case we expect the I-V shape to be closer to the realistic one due to better statistics. For completeness, we use another variation of the classical

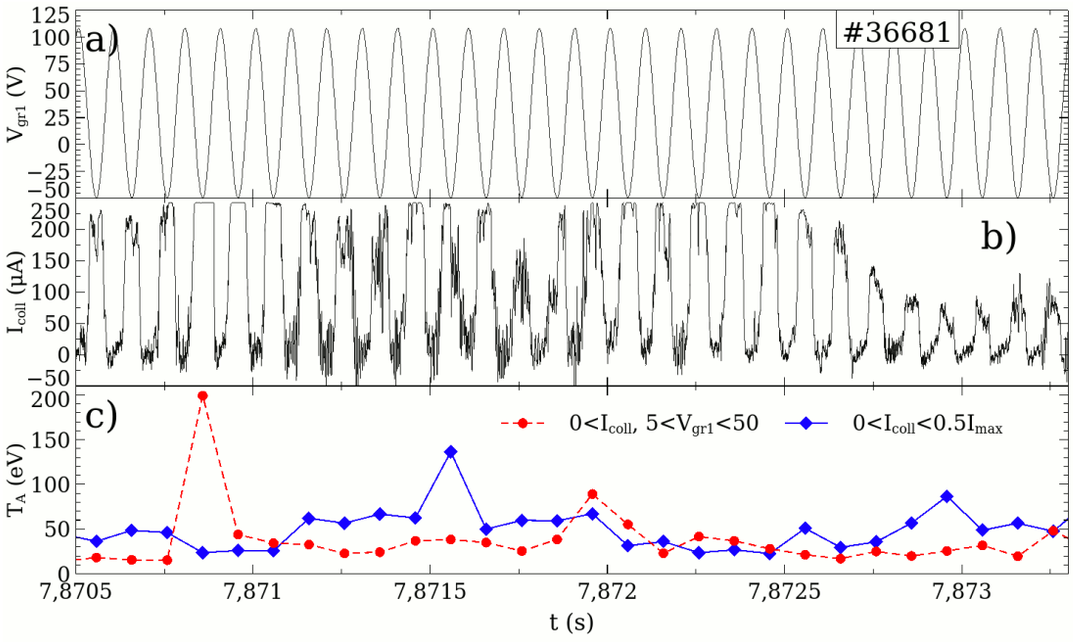

Figure 8: (a) The RFA2 grid 1 voltage V_{gr1} and (b) the collector current I_{coll} in discharge #36681. A 10 kHz sweeping frequency is used. The RFA2 position is fixed. (c) The time evolution of the ion temperature measured by the Side A analyzer, calculated using two fitting criteria.

conditional averaging method, where averaging is applied *after* taking the natural logarithm of the raw collector current data. Implementation of this technique to the 100 Hz and 10 kHz data cases is shown in Fig. 10. This technique gives rather similar I-V characteristics. As it is seen from the I-V

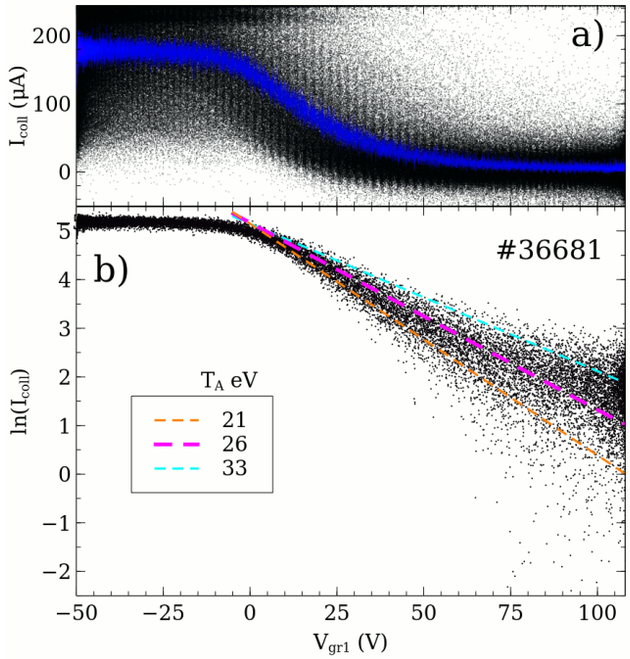

Figure 9: The RFA2 I-V curve in discharge #36681. Data from a 30 ms time window is plotted on (a) a linear and (b) a logarithmic scale. Raw data in (a) is shown by black dots and conditionally averaged data is shown by blue lines. The Side A analyzer is used. The estimated T_i value is 26 eV, or 21-33 eV within the error bars.

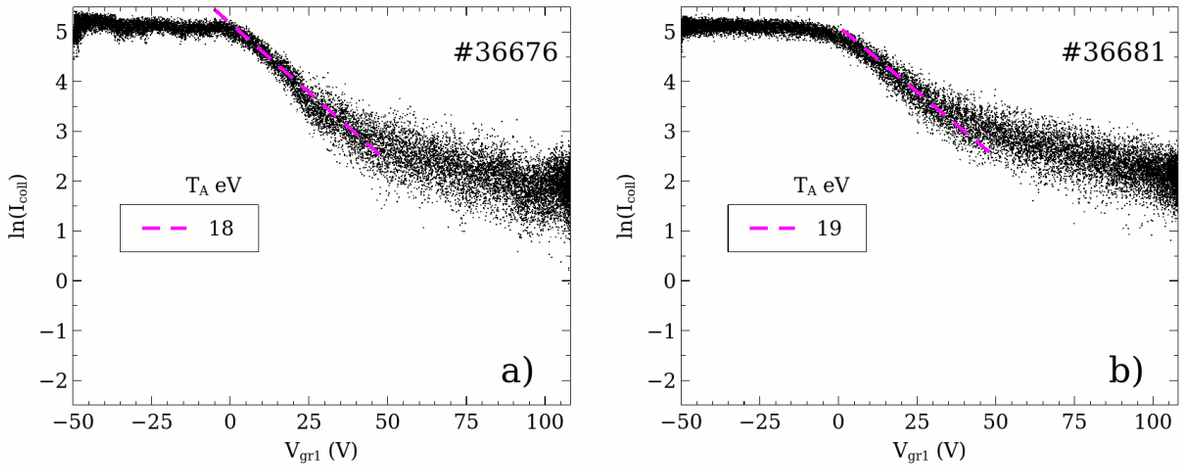

Figure 10: The I-V characteristics of the RFA2 data with grid 1 voltage sweeps at (a) 100 Hz (#36676) and (b) 10 kHz (#36681). I_{coll} data from a 30 ms time window is plotted on a logarithmic scale. Negative collector currents are removed from the signals. Conditional averaging is applied *after* taking the natural logarithm of the data. The Side A analyzer is used.

characteristics, only 5-50 V part of the slope can be described by a single ion temperature. This fact represents the noisy nature of the collector current signal for V_{gr1} in the range of 50-100 V. As a result, this part of the I-V curve is removed from our analysis. The average ion temperature measured by the Side A analyzer is 18-19 eV in these cases (Fig. 10), which is lower than the values of 23-26 eV in Figs. 6 and 9. The difference is attributed to how the bipolar amplifier noise (visible in Fig. 4 (a)) distorts the statistical distribution of the collector current signal. Advantages or disadvantages of these two approaches depend on the electronics noise character of the RFA collector signal. In the case of a symmetric bipolar noise, its influence can be suppressed via conditional averaging as shown in Figs. 6 and 9. However, applying conditional averaging after we take the natural logarithm of the collector current data fails to properly subtract the symmetric electronics noise. As a result, the technique of data description shown in Figs. 6 and 9 is usually implemented for the RFA data analysis. Next we show that in the case of a strongly intermittent plasma the classical conditional averaging approach should be replaced by the use of the most probable quantities.

A different approach to analyze intermittent signals is based on the implementation of a straight forward statistical method. At every sweeping grid 1 voltage region we can compute the most probable value of the RFA collector current signal, as it is shown in Fig. 11. At this point we can

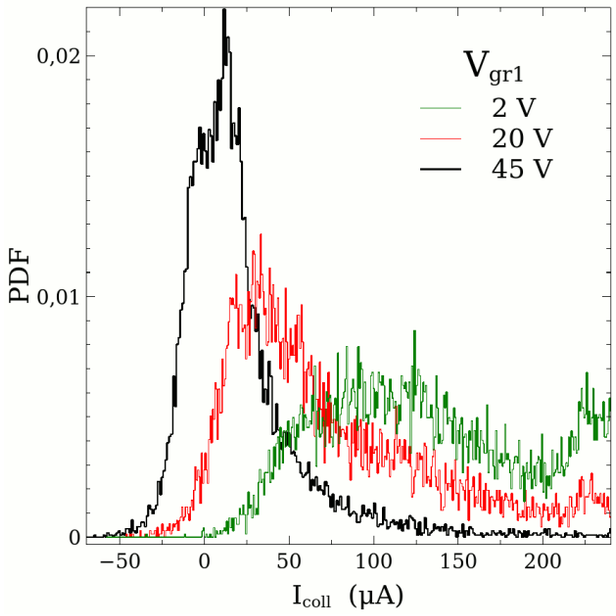

Figure 11: The probability density function of the RFA collector current signal for three different grid 1 voltages (the values are marked in the legend).

introduce additional filters for spurious I_{coll} signal spikes (for example, saturated I_{coll} peaks). We can use the most probable values of I_{coll} for I-V reconstruction, as shown in Fig. 12. In this case the I-V curve represents the distribution of the most probable values in contrast to the averaged values in the conventional methods. The methods show rather different slopes, due to the substantial difference between the most probable and the mean values in the RFA I_{coll} data. We can see from Fig. 11 that the I_{coll} PDF is not symmetric about its maximum, but follows a Gamma-like shape. This causes the difference between the mean and the most probable values. The I-V characteristics based on the most probable method is fitted to give us 15 eV, in contrast to the 26 eV ion temperature according to the classical conditional averaging method. The time-averaged techniques of the RFA ion temperature estimation are considered for cross-validation of slow and fast sweeping modes of RFA operations. Both fast and slow sweeping modes produce rather similar mean ion temperatures following the same procedures of data processing. However, in the case of intermittent I_{coll} signals without a constant component, the classical description of the plasma via the mean ion temperature becomes ambiguous.

As we show in Fig. 12, the mean-based and the most probable-based I-V methods produce quite different results. A more accurate description of the intermittent plasma is based on the statistics of the ion temperature distribution calculated in every RFA V_{gr1} sweep during fast sweeping operation, as it is described in the next section.

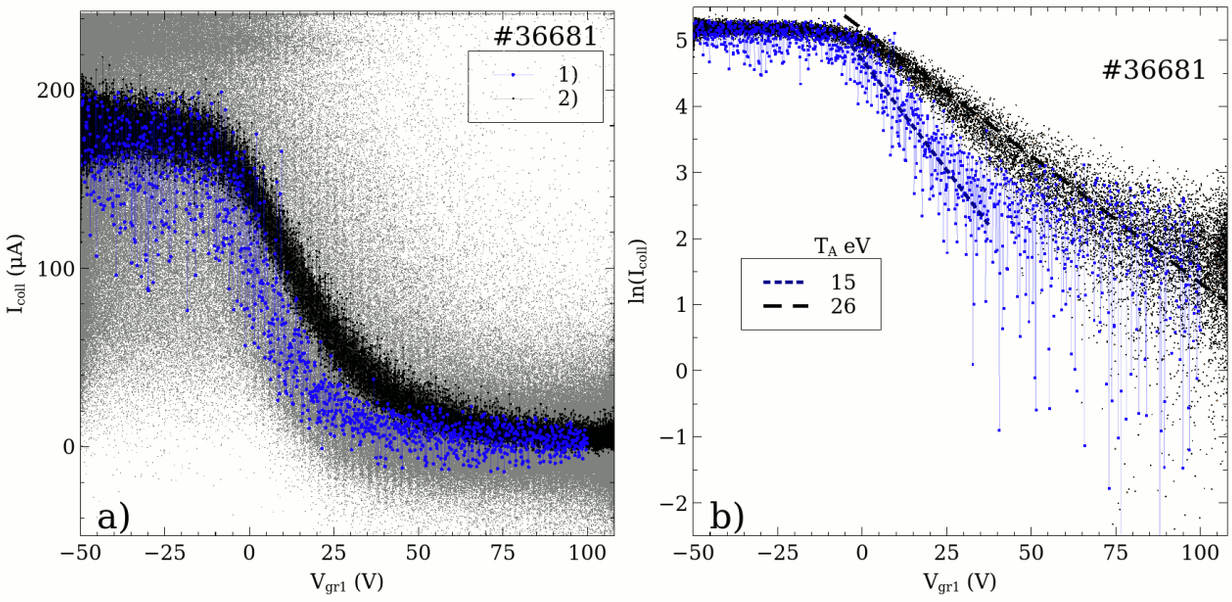

Figure 12: The I-V characteristics of RFA2 using: 1) the PDF and 2) conditional averaging. The I-V characteristics are plotted on (a) a linear scale and (b) a logarithmic scale. The Side A analyzer is used. Shown raw data is from a 30 ms time window of #36681.

4.2. Techniques for RFA ion temperature estimation via PDF

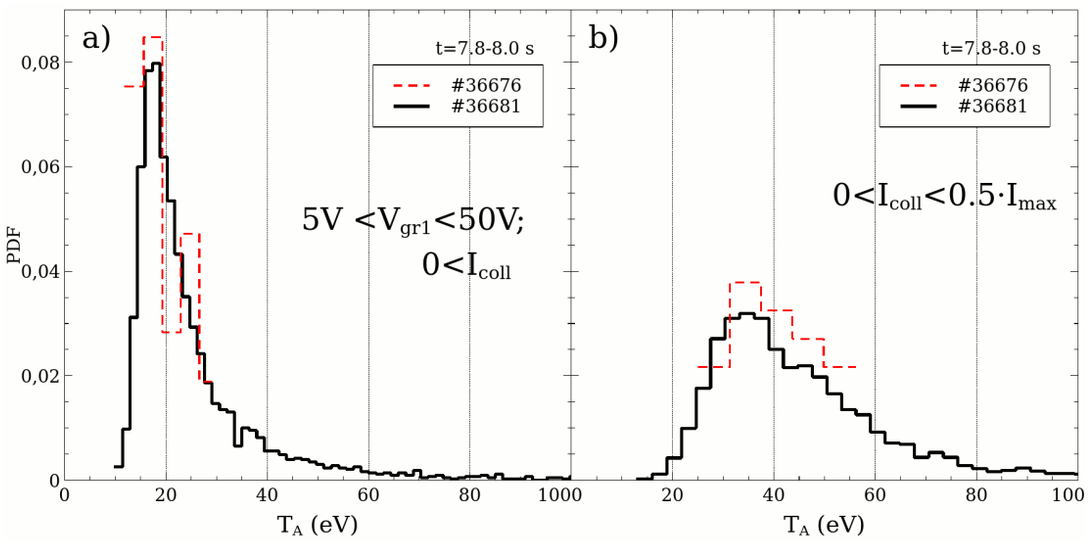

Figure 13: The PDFs of the ion temperature produced using two boundary conditions: (a) $5 < V_{gr1} < 50$ V and $I_{coll} > 0$, which effectively averages over fluctuations; and (b) $0 < I_{coll} < 0.5 I_{max}$, which follows fluctuations. The PDFs are computed for slow (#36676) and fast (#36681) V_{gr1} sweeps. The Side A analyzer is used.

In the case of fast RFA sweeping, we can calculate the ion temperature for every half-period of the RFA grid 1 voltage sweep. The ion temperature now can be described by the PDF, which is reconstructed from a large set of I-V characteristics. The reconstructed PDF is sensitive to the applied boundary conditions that we use when computing T_i from the I-V data, as explained next. The plasma potential, the ion temperature, and the plasma density fluctuations can affect RFA measurements. These fluctuations modify the RFA grid 1 voltage region, where the collector current slope is located. In the case of slow techniques, these fluctuations cannot be individually resolved. If we compute the slope only from the I-V region where $I_{coll} > 0$ and $5 < V_{gr1} < 50$ V, we effectively ignore I_{coll} fluctuations. As a result, we expect that the reconstructed PDF using these boundary conditions should provide T_i values similar to the classical conditional averaging results because the fluctuations are ignored in both cases.

Alternatively, we can compute the slope by following the fluctuations of the collector current signal. For example, if we compute the slope only from the I-V region bounded by $0 < I_{coll} < 0.5I_{max}$, where I_{max} is the maximum RFA collector current during this half of period, we effectively track or follow the plasma fluctuations. Ion temperature distributions computed using the above-mentioned two boundary conditions (from the Side A analyzer) are shown in Fig. 13. As we see from Fig. 13, the most probable temperatures are reproduced in the cases of slow (#36676) and fast (#36681) grid 1 voltage sweeps. The fast sweeping technique provides more data and the PDF contains more details in this case. In the case of the first boundary condition (Fig. 13 (a)), the most probable temperature of 17-19 eV is rather similar to the conventional technique of conditionally averaged I-V analysis described in the previous section (Figs. 6 and 9). This fact represents a similar approach to the data analysis – in both methods the fast fluctuations of the RFA collector current slope are ignored. In the case of the second boundary condition (Fig. 13 (b)), the most probable temperature of 30-37 eV is substantially higher. This difference represents the influence of the strong fluctuations of the plasma density, the ion temperature and the potential in the intermittent H-mode plasma of ASDEX Upgrade. Due to the fast enough sweeping time, we can track these fluctuations via measured RFA I-V modifications. We should note, that the 100 Hz sweeping frequency is not fast enough in comparison with the typical ELM cycle time (Fig. 7). For completeness, we show that the results measured with the Side A analyzer are reproduced when using the Side B analyzer of the RFA2 diagnostic (Fig. 14). Higher RFA temperature from side B represent a well-known influence of the plasma flow on the RFA measurement [15, 23]. The two boundary conditions consistently show higher ion temperatures from the Side B analyzer. The second boundary condition ($0 < I_{coll} < 0.5I_{max}$) gives a higher ion temperature on both Side A and Side B analyzers. We can estimate the "actual" ion temperature by taking the average value as: $T_i = 0.5(T_A+T_B)$ [15, 23]. The most probable ion temperature, according to the second boundary condition is about 50 eV. This rather high ion temperature is convected to the SOL by the ELM filaments. Due to the low plasma density in the SOL in our discharges, ion cooling is slow, hence, allowing for the high T_i values near the limiter.

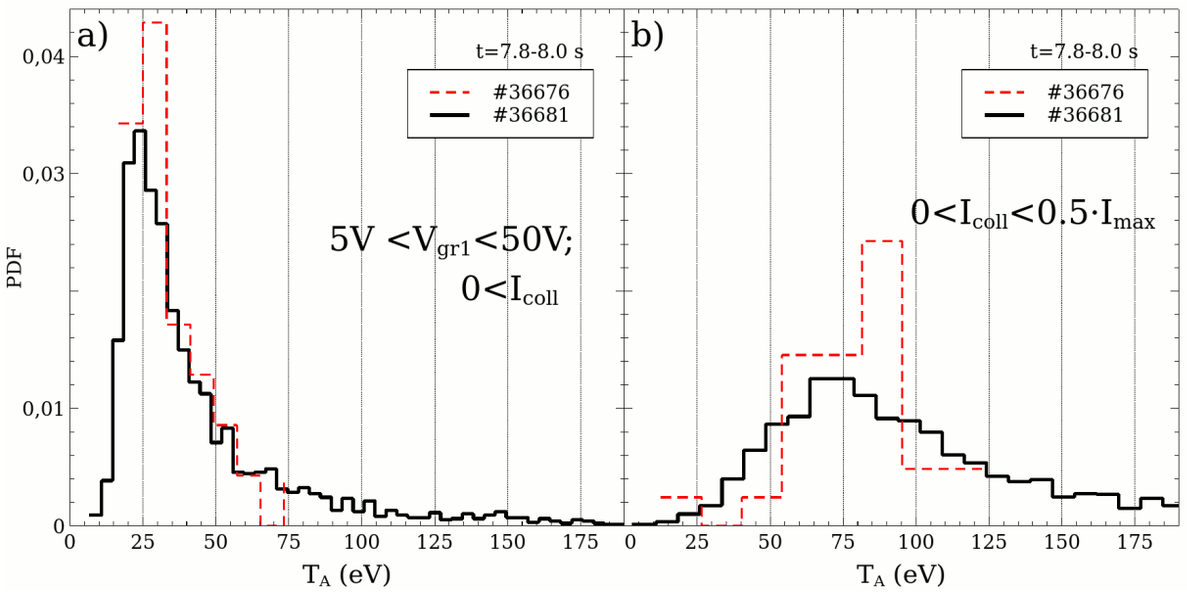

Figure 14: The PDFs of the ion temperature produced using two boundary conditions: (a) $5 < V_{gr1} < 50$ V and $I_{coll} > 0$, which effectively averages over fluctuations; and (b) $0 < I_{coll} < 0.5I_{max}$, which follows fluctuations. The PDFs are computed for slow (#36676) and fast (#36681) V_{gr1} sweeps. The Side B analyzer is used.

5. Summary and conclusions

Fast measurements and statistical methods are desirable to adequately describe fast random events caused by ELMs and blobs in the SOL plasmas. A new diagnostic method to interpret the Retarding Field Analyzer (RFA) measurement in strongly intermittent plasmas is proposed and tested in ASDEX Upgrade H-mode plasmas. Fast sweeping of the RFA grid 1 voltage with the sweeping rate of 10 kHz is used. We also use a capacitance compensated circuit when measuring the RFA collector current to minimize the I-V distortion due to the connecting cable capacitance (Figs. 3 and 4). Conventional RFA data analysis techniques based on the conditionally averaged (or mean) RFA I-V characteristics during a long time interval are presented (Figs. 6 and 9). The methods are compared between slow (100 Hz) and fast (10 kHz) sweeping cases of the RFA grid 1 voltage. This comparison shows that the sweeping rate does not change the resulting ion temperature measurements. However, the choice of a particular technique does impact the resulting T_i values. The differences between the various techniques are attributed to the effect of plasma fluctuations on the I-V profiles. Our proposed solution to overcome the effect of plasma fluctuations is to perform fast (10 kHz) sweeps for I-V characteristic generation and then use a statistical approach to reconstruct the probability density function (PDF) of the ion temperature. We observe that the PDF method does depend on the boundary conditions applied to the I_{coll} and V_{gr1} values when estimating T_i from the I-V characteristics. If the boundary conditions are insensitive to the fluctuations ($I_{coll} > 0$ and $5 < V_{gr1} < 50$ V), then the most probable T_i value from the PDF method coincides with the T_i value from the classical mean technique (Figs. 6, 9, and 13 (a)). However, if the boundary conditions are such that they follow the fluctuations ($0 < I_{coll} < 0.5I_{max}$), the PDF method gives T_i values much higher than the conditional averaging method (Fig. 13 (b)). Even if the sweeping rate is not fast enough and the temporal evolution of the I-V characteristics remains partially disturbed by the fluctuations, the distributions remain compensated statistically due to the random nature of fluctuations (Fig. 13, shot #36676 curves). The substantially higher T_i values (Fig. 13 (b)) are reproduced on both analyzer sides of the RFA2 diagnostic (Fig. 14 (b)). These high T_i values are attributed to reduced ion cooling in the low plasma density far SOL region. Overall, we show that a fast sweeping RFA diagnostic in combination with a PDF data analysis method should be used in intermittent SOL plasmas to provide accurate T_i measurements.

Acknowledgements
This work has been carried out within the framework of the EUROfusion Consortium and has received funding from the Euratom research and training programme 2014-2018 and 2019-2020 under grant agreement No 633053. The views and opinions expressed herein do not necessarily reflect those of the European Commission. Martin Kočan's contribution to the initial development of the RFA2 diagnostic on ASDEX Upgrade is acknowledged.

Data availability
The data that support the findings of this study are available from the corresponding author upon reasonable request.

References
[1] S. J. Zweben, the Physics of Fluids 28, 974 (1985).
[2] H. Zohm, Plasma Phys. Control. Fusion 38 (1996) 105-128.
[3] J. L. Terry, S. J. Zweben, K. Hallatschek, B. LaBombard, R. J. Maqueda, B. Bai, C. J. Boswell, M. Greenwald, D. Kopon, W. M. Nevins, et al. Physics of Plasmas 10, 1739 (2003).
[4] S. J. Zweben, R. J. Maqueda, J. L. Terry, T. Munsat, J. R. Myra, D. D'Ippolito, D. A. Russell, J. A. Krommes, B. LeBlanc, T. Stoltzfus-Dueck, et al., Physics of Plasmas 13, 056114 (2006).

[5] O. E. Garcia, I. Cziegler, R. Kube, B. LaBombard, J. L. Terry, Journal of Nuclear Materials 438, S180-S183 (2013).
[6] G. Y. Antar, M. Tsalas, E. Wolfrum, V. Rhode, Plasma Phys. Control. Fusion 50, 095012 (2008).
[7] M. Dreval, M. Hubeny, Y. Ding, T. Onchi, Y. Liu, K. Hthu, S. Elgriw, C. Xiao and A. Hirose, Plasma Phys. Control. Fusion 55, 035004 (2013).
[8] I. Langmuir, Physical Review, 2:450–486, 1913.
[9] G. Chiodini, C. Riccardi, and M. Fontanesi, Review of Scientific Instruments 70, 2681 (1999).
[10] H.W. Müller, J. Adamek, J. Horacek, C. Ionita, F. Mehlmann, V. Rohde, R. Schrittwieser, Contrib. Plasma Phys. 50, No. 9, 847 – 853 (2010).
[11] Sin-Li Chen and T. Sekiguchi, Journal of Applied Physics 36, 2363 (1965).
[12] J. Adámek, J. Stöckel, I. Ďuran, M. Hron, R. Pánek, M. Tichý, R. Schrittwieser, C. Ionit, P. Balan, E. Martines & G. Van Oost, Czechoslovak Journal of Physics, 55, 235–242 (2005).
[13] H. Y. Guo, G. F. Matthews, S. J. Davies, S. K. Erents, L. D. Horton, R. D. Monk, P. C. Stangeby Contrib. Plasma Phys. 36 (1996) S, 81-86.
[14] D. Brunner, B. LaBombard, R. Ochoukov, and D. Whyte, Rev. Sci. Instr. 84, 033502 (2013).
[15] M. Dreval, D. Rohraff, C. Xiao, and A. Hirose, Rev. Sci. Instr. 80, 103505 (2009).
[16] M. Kočan, S.Y. Allan, S. Carpentier-Chouchana, P. de Marné, S. Elmore, T. Franke, J.P. Gunn, A. Herrmann, A. Kirk, M. Kubič, et al., Nuclear Fusion 52, 023016 (2012).
[17] M. Henkel, Y. Li, Y. Liang, P. Drews, A. Knieps, C. Killer, D. Nicolai, D. Hoeschen, J. Geiger, C. Xiao, et al., Fusion Engineering and Design 157, 111623 (2020).
[18] S. Elmore, S. Y. Allan, G. Fishpool, A. Kirk, A. J. Thornton, N. R. Walkden, J. R. Harrison, Plasma Phys. Control. Fusion 58 (2016) 065002.
[19] I. S. Nedzelskiy, C. Silva, P. Duarte, and H. Fernandes, Rev. Sci. Instrum. 82, 043505 (2011).
[20] I. S. Nedzelskiy, C. Silva, and H. Fernandes, Rev. Sci. Instrum. 85, 093506 (2014).
[21] http://www.flcelectronics.com/
[22] K.Behler, H. Blank, H. Eixenberger, M. Fitzek, A. Lohs, K. Lueddecke, R. Merkel, Fusion Engineering and Design, 87 (2012) 2145-2151.
[23] F. Valsaque, G. Manfredi, J. P. Gunn, and E. Gauthier, Phys. Plasmas 9, 1806 (2002).

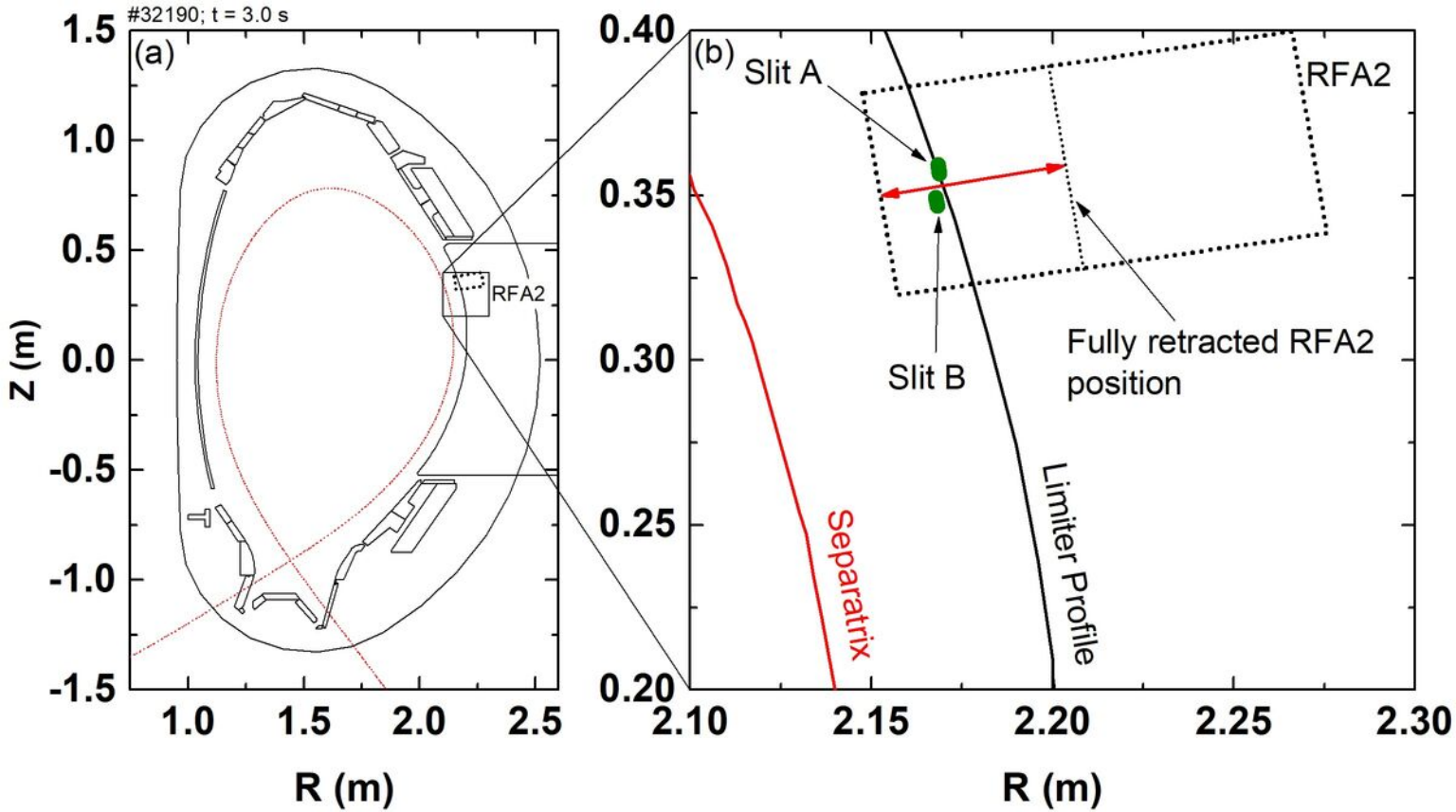
#32190; t = 3.0 s
(a)
RFA2
Z (m)
R (m)
(b)
Slit A
Slit B
RFA2
Fully retracted RFA2 position
Separatrix
Limiter Profile
R (m)

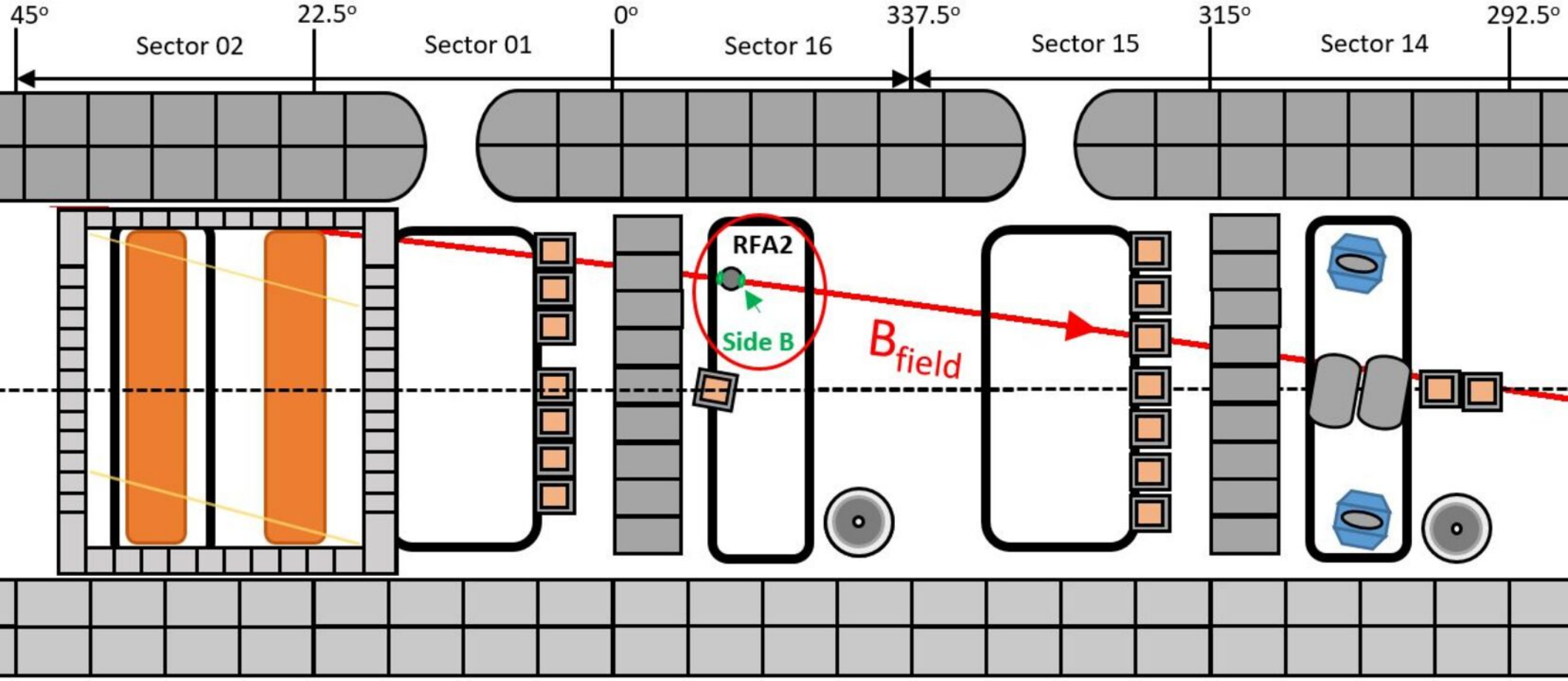
45°
22.5°
0°
337.5°
315°
292.5°
Sector 02
Sector 01
Sector 16
Sector 15
Sector 14
RFA2
Side B
B_{field}

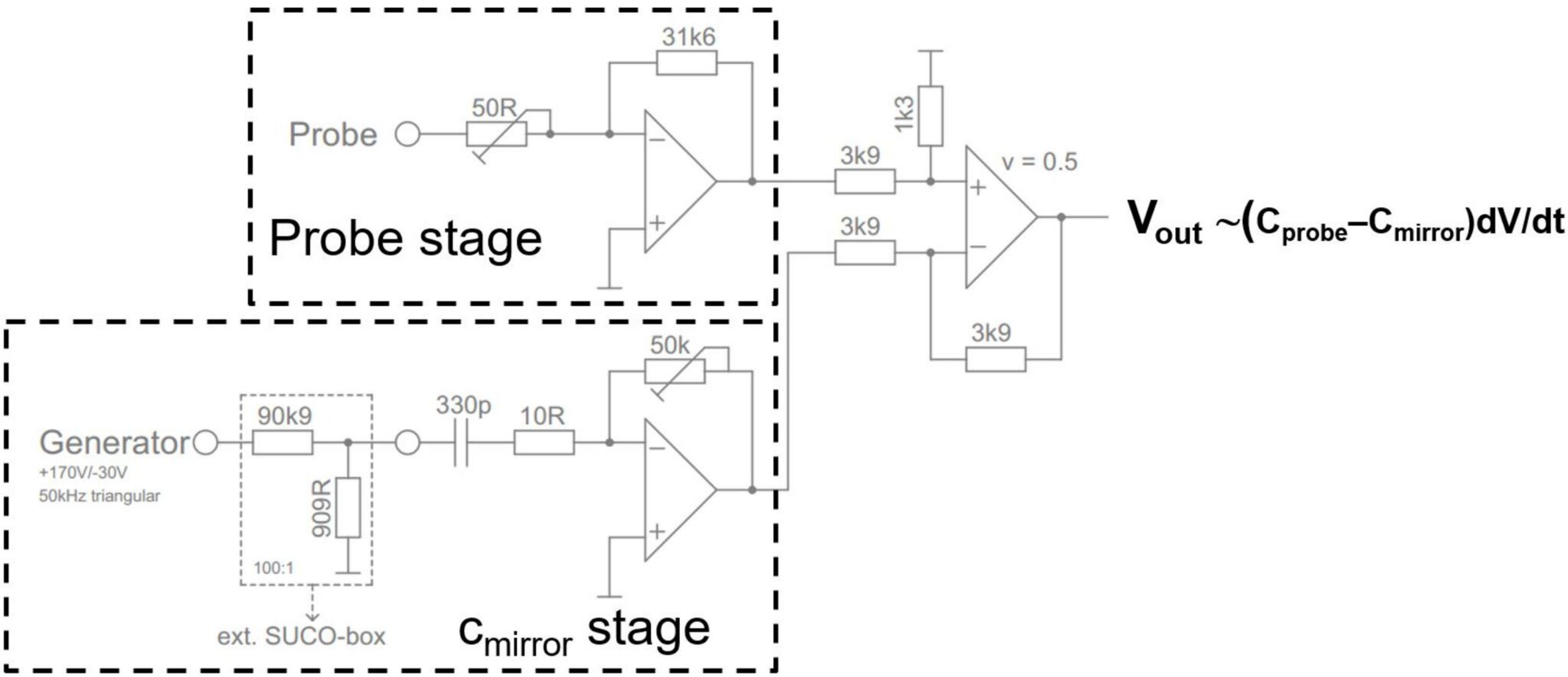
31k6
50R
Probe
Probe stage
1k3
3k9
3k9
v = 0.5
$V_{out} \sim (C_{probe} - C_{mirror}) dV/dt$
3k9
50k
330p
10R
90k9
Generator
+170V/-30V
50kHz triangular
909R
100:1
ext. SUCO-box
C_{mirror} stage

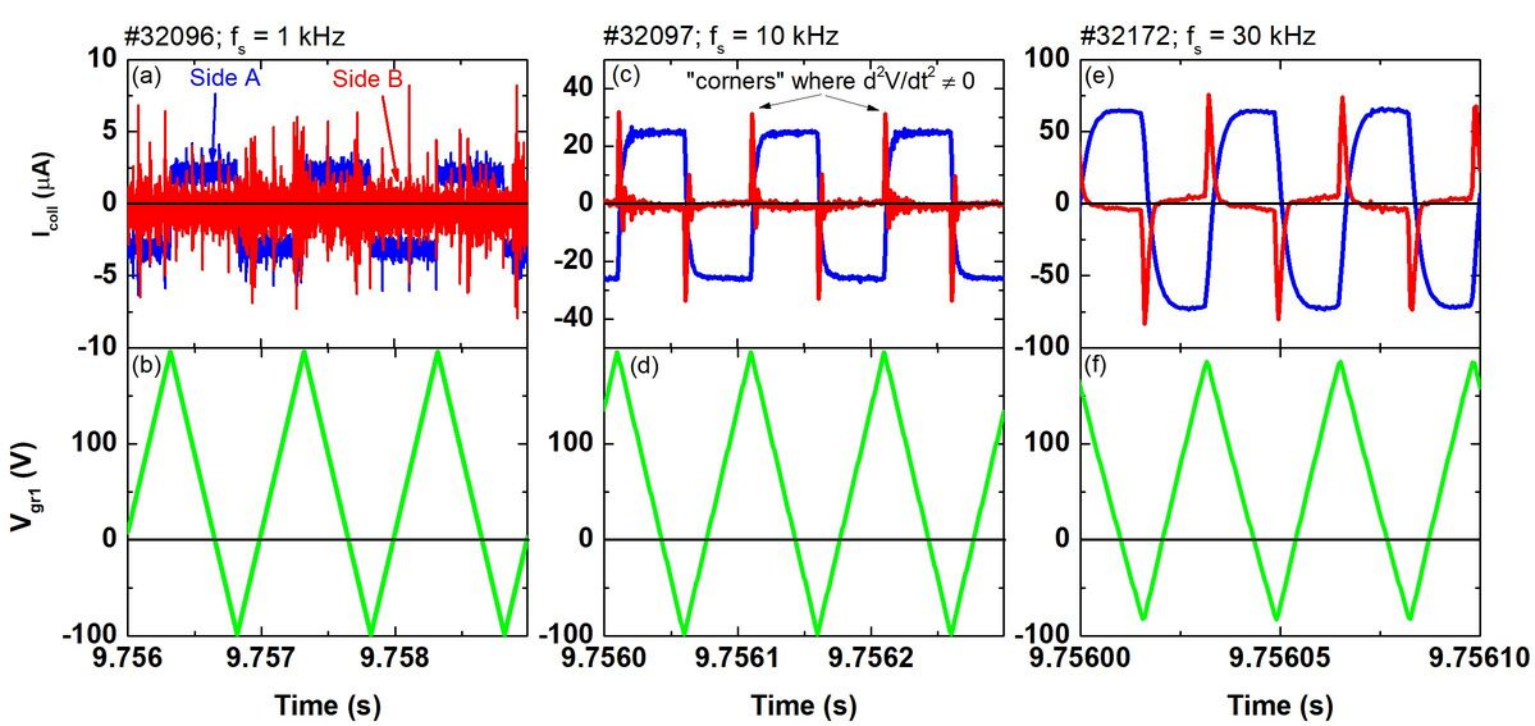
#32096; f_s = 1 kHz
#32097; f_s = 10 kHz
#32172; f_s = 30 kHz
(a)
Side A
Side B
(c)
"corners" where d²V/dt² ≠ 0
(e)
(b)
(d)
(f)
I_coil (μA)
V_gr1 (V)
Time (s)
Time (s)
Time (s)

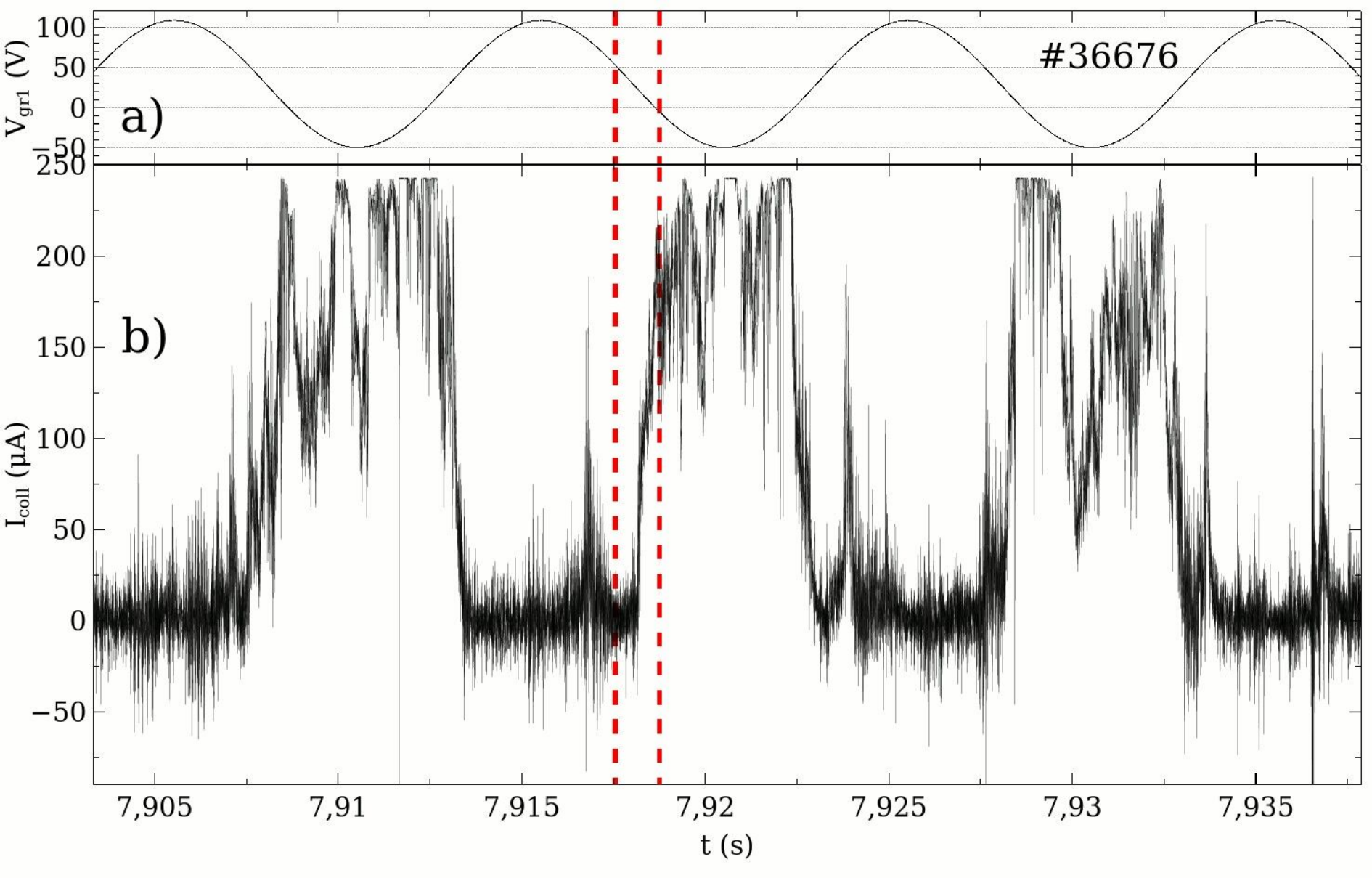
#36676
a)
b)
V_{gr1} (V)
I_{coll} (μA)
100
50
0
−50
250
200
150
100
50
0
−50
7,905
7,91
7,915
7,92
7,925
7,93
7,935
t (s)

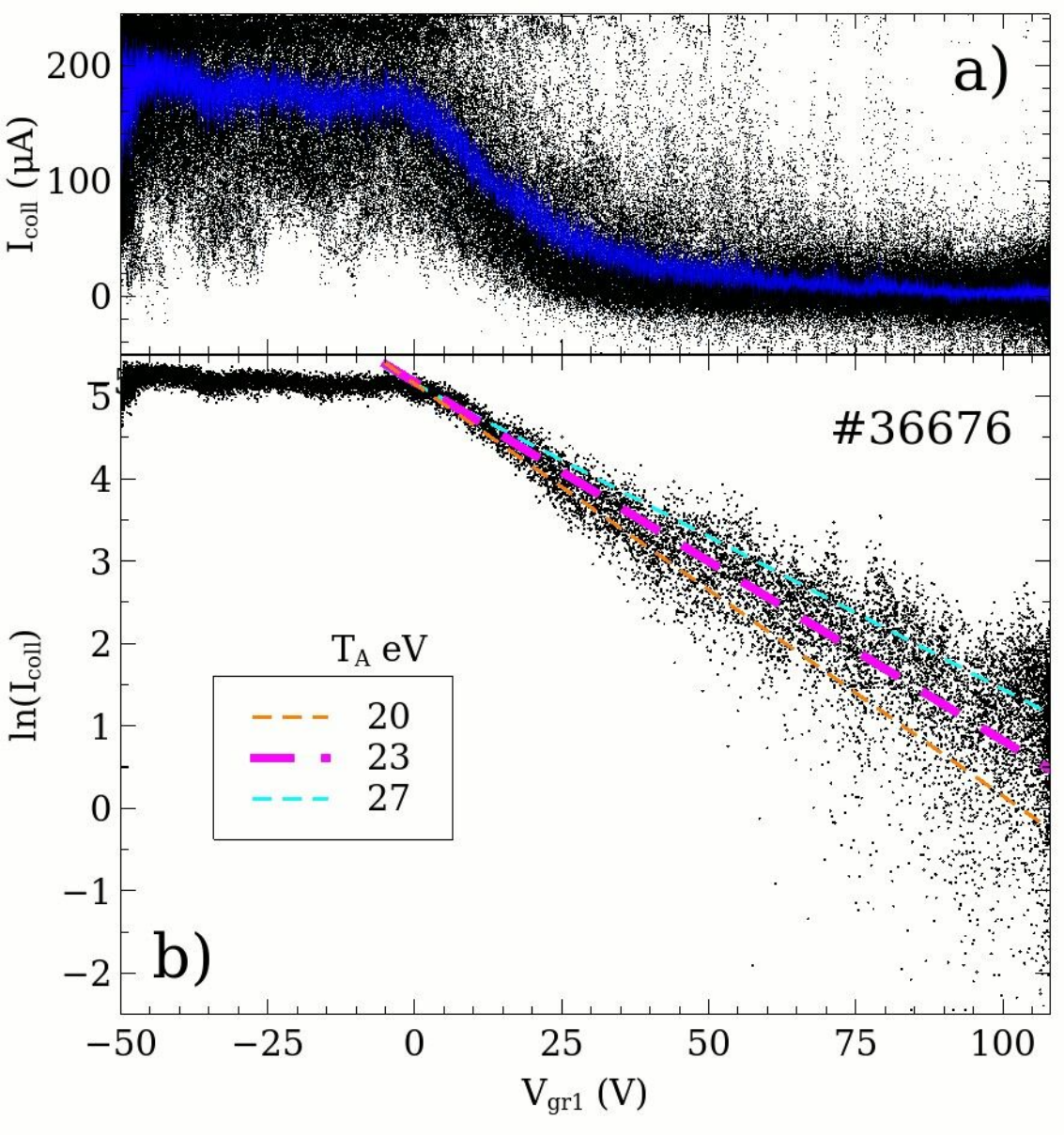
a)
200
100
0
I_{coll} (μA)
#36676
5
4
3
2
1
0
−1
−2
$\ln(I_{coll})$
T_A eV
20
23
27
b)
−50
−25
0
25
50
75
100
V_{gr1} (V)

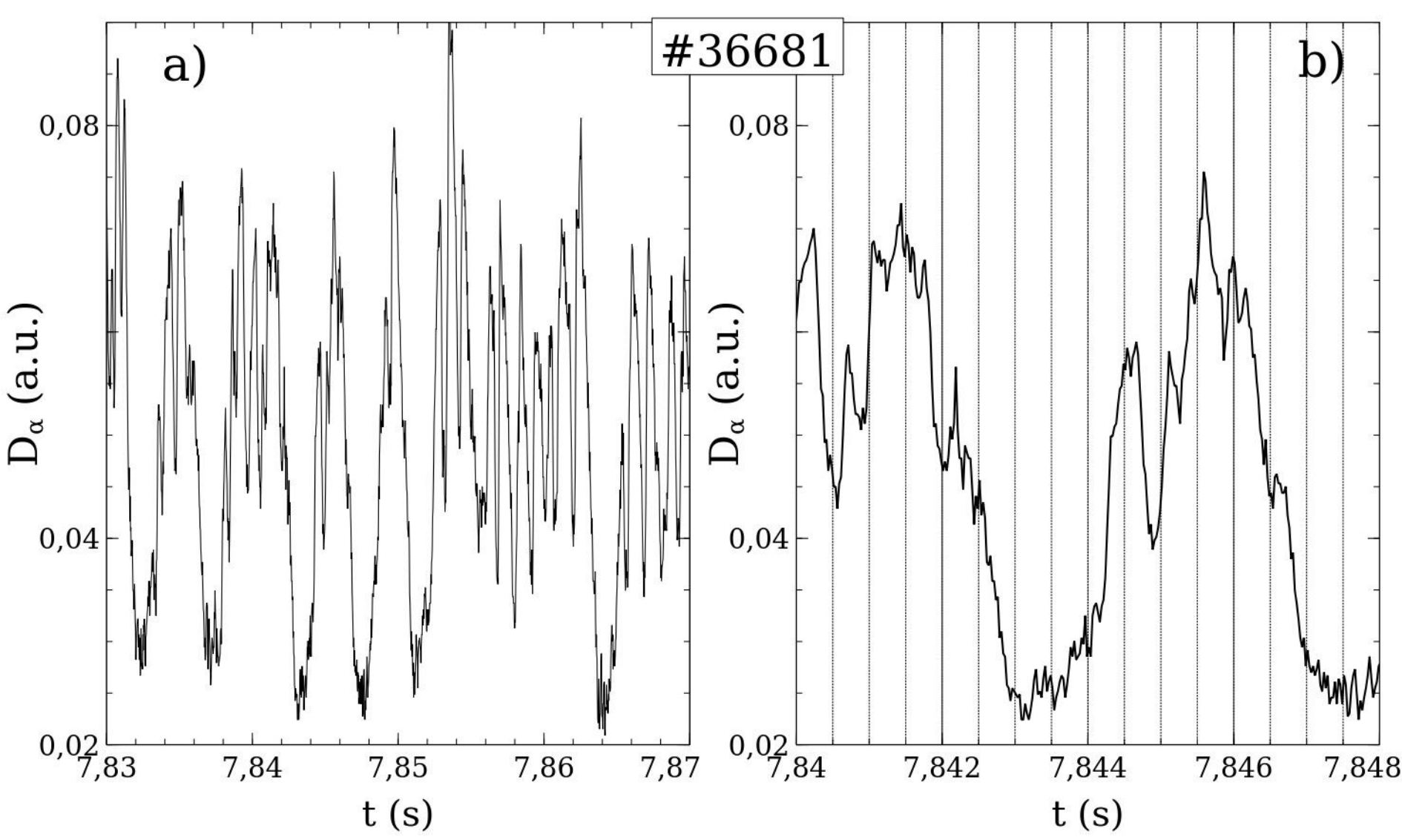
#36681
a)
b)
0,08
0,04
0,02
D_α (a.u.)
7,83
7,84
7,85
7,86
7,87
7,842
7,844
7,846
7,848
t (s)

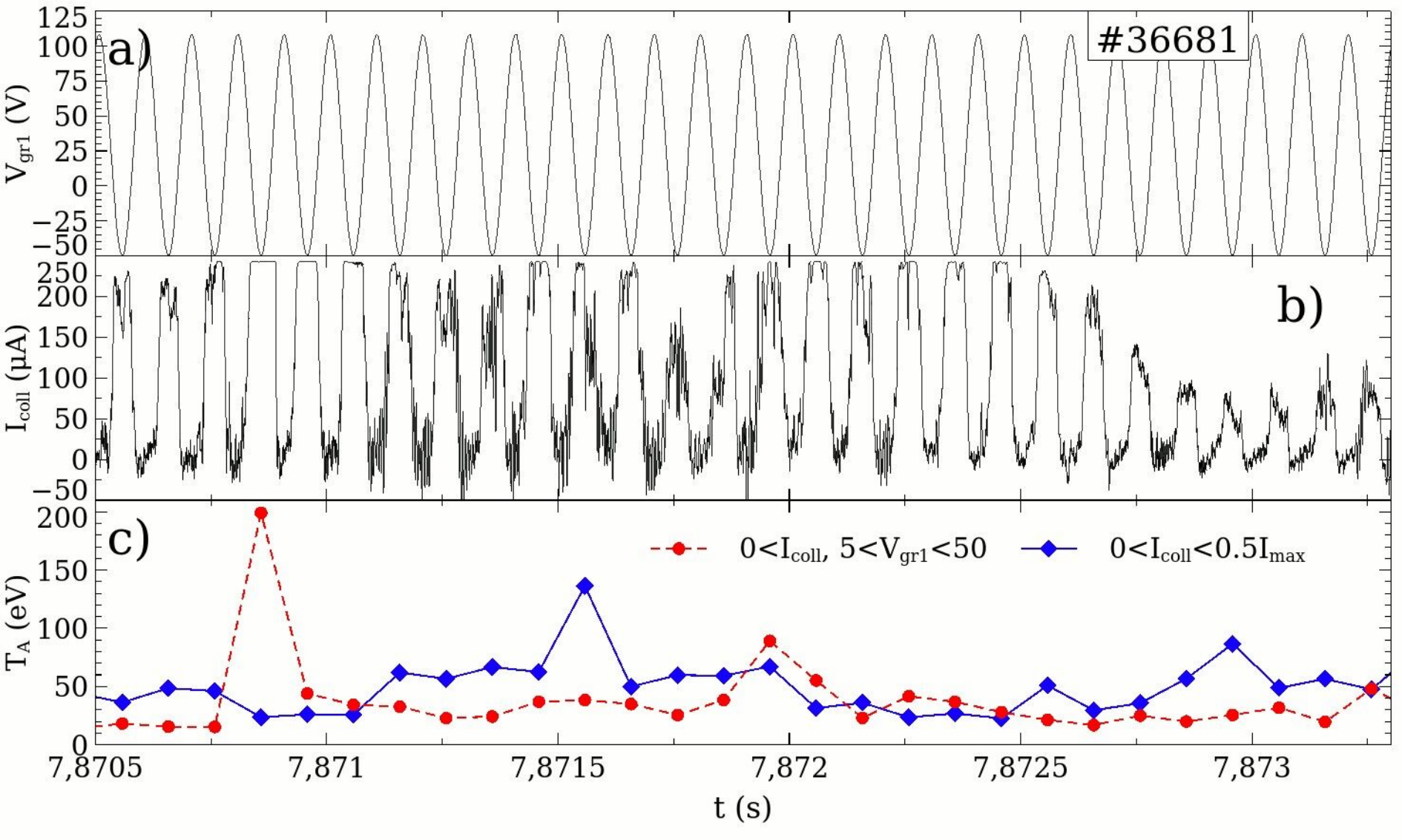
a)
#36681
V_{gr1} (V)
b)
I_{coll} (μA)
c)
T_A (eV)
$0<I_{coll}$, $5<V_{gr1}<50$
$0<I_{coll}<0.5I_{max}$
t (s)

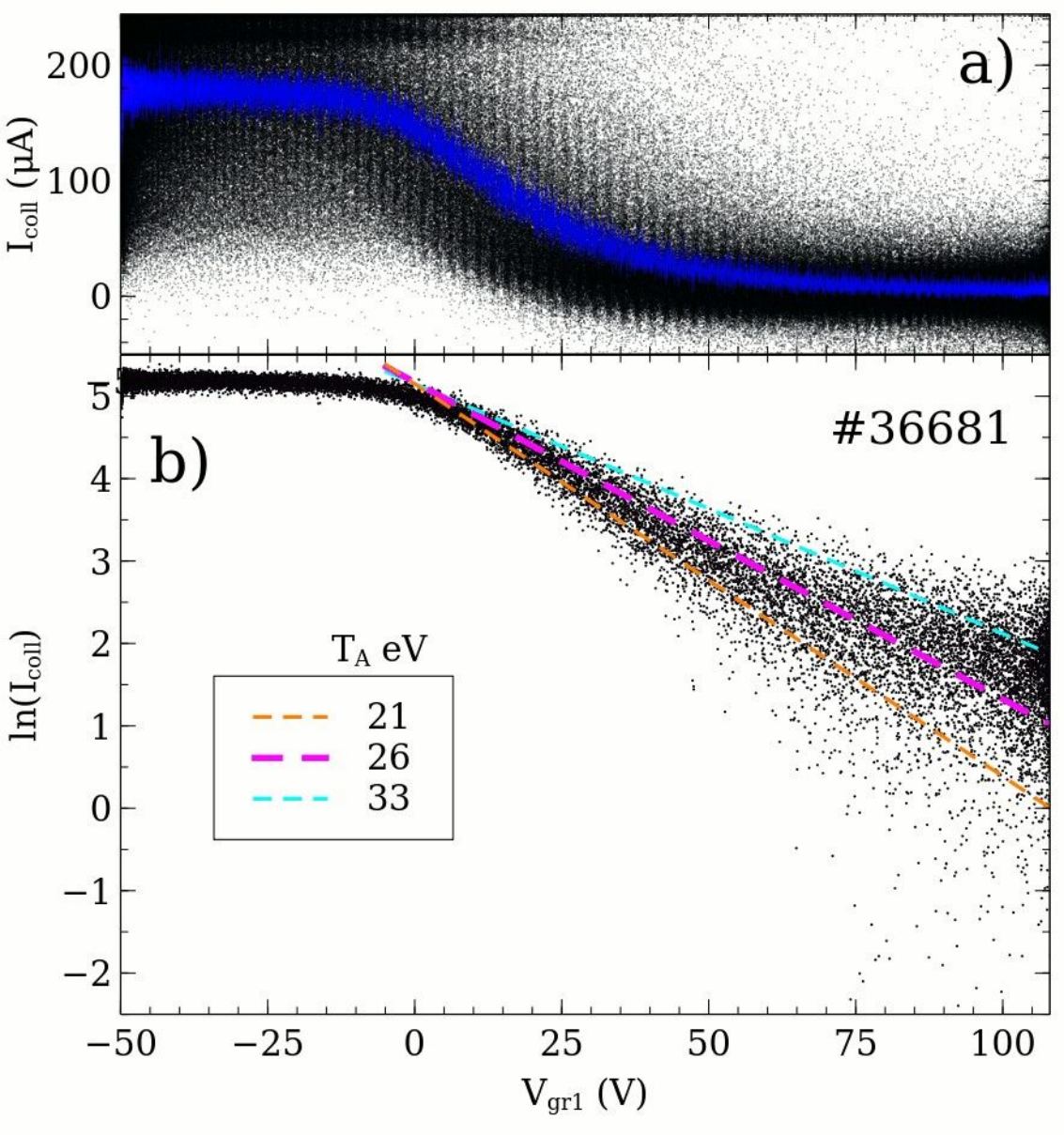
a)
b)
#36681
I_{coll} (μA)
200
100
0
$\ln(I_{coll})$
5
4
3
2
1
0
−1
−2
T_A eV
21
26
33
−50
−25
0
25
50
75
100
V_{gr1} (V)

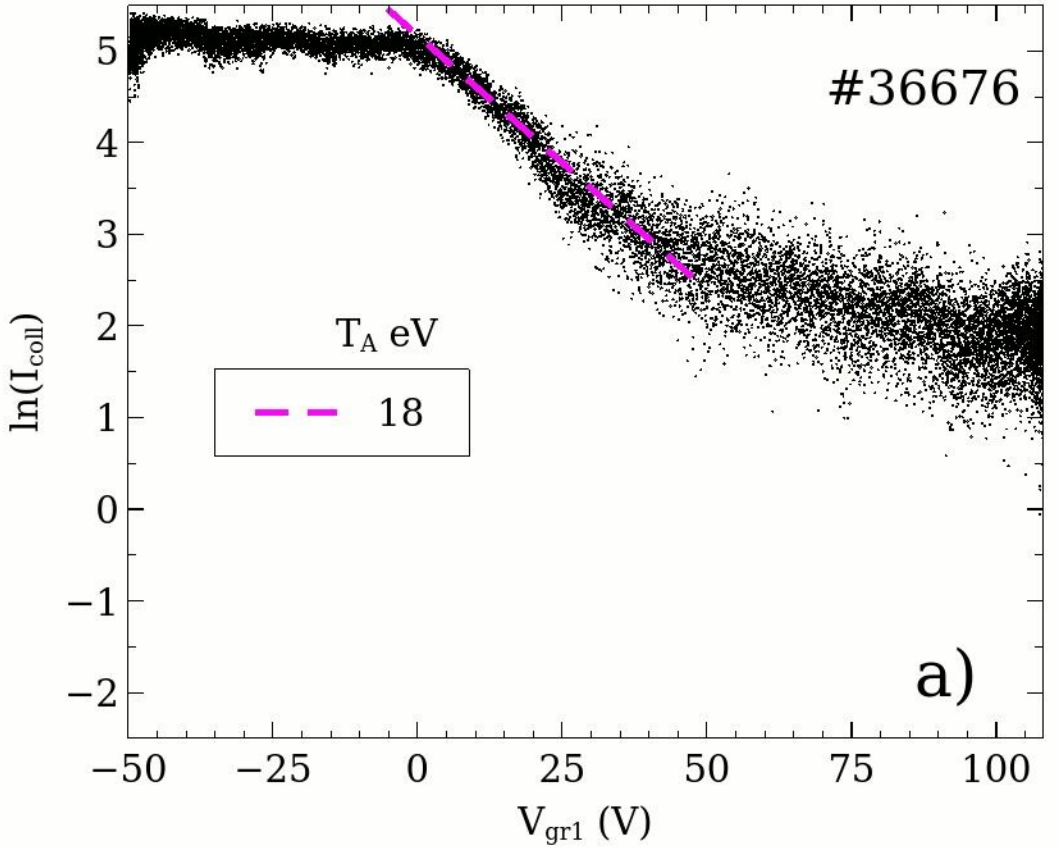
#36676
T_A eV
18
a)
$\ln(I_{coll})$
V_{gr1} (V)

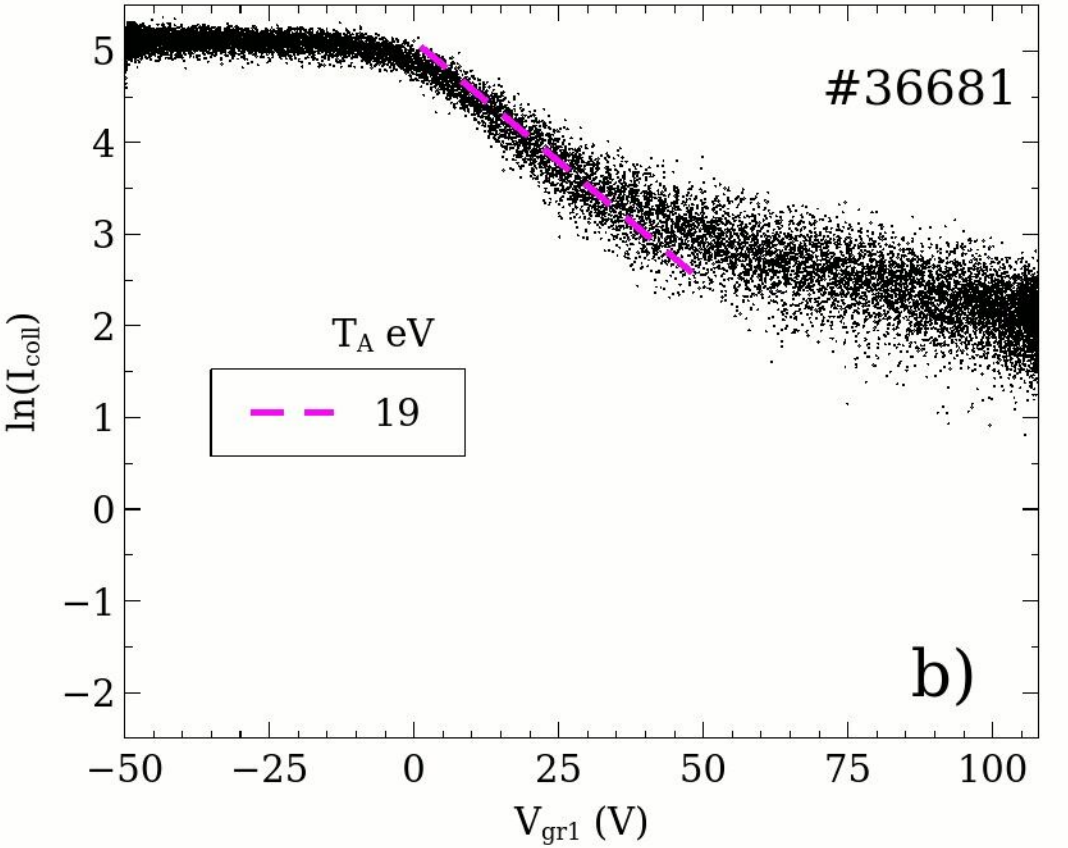
#36681
T_A eV
19
b)
$\ln(I_{coll})$
V_{gr1} (V)

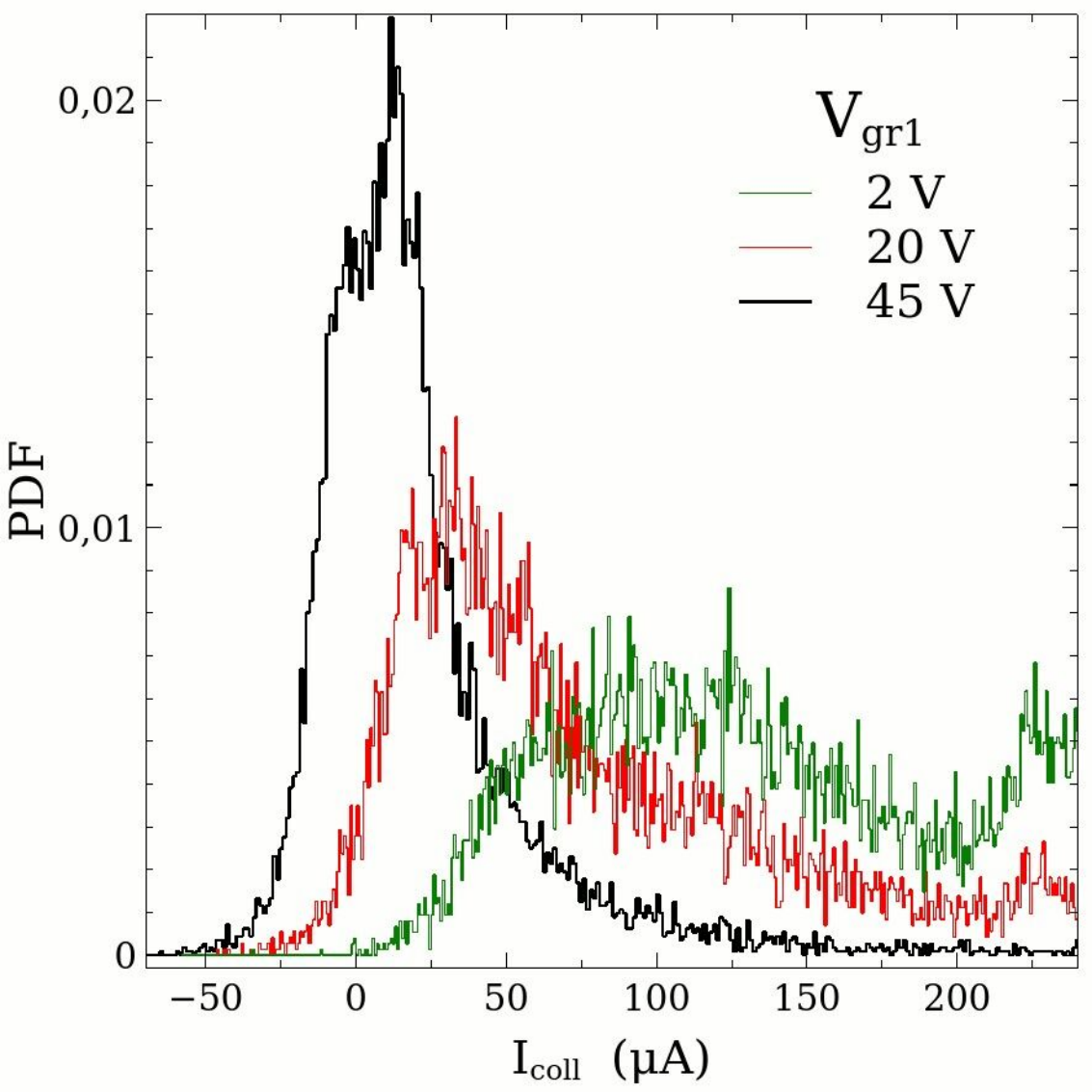
0,02
0,01
0
PDF
V_{gr1}
2 V
20 V
45 V
−50
0
50
100
150
200
I_{coll} (μA)

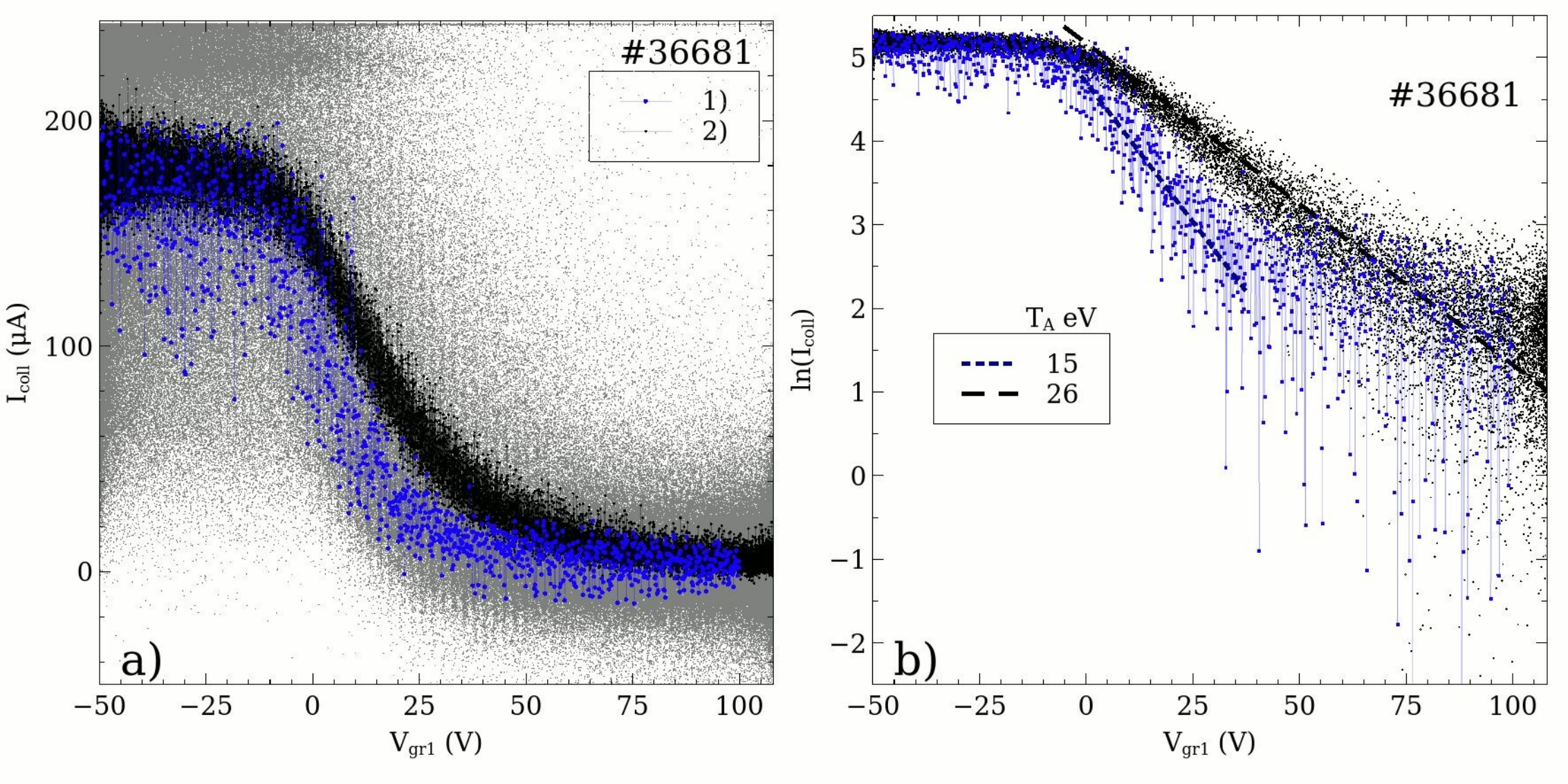
#36681
1)
2)
200
100
0
I_{coll} (μA)
a)
−50
−25
0
25
50
75
100
V_{gr1} (V)
#36681
T_A eV
15
26
5
4
3
2
1
0
−1
−2
ln(I_{coll})
b)
−50
−25
0
25
50
75
100
V_{gr1} (V)

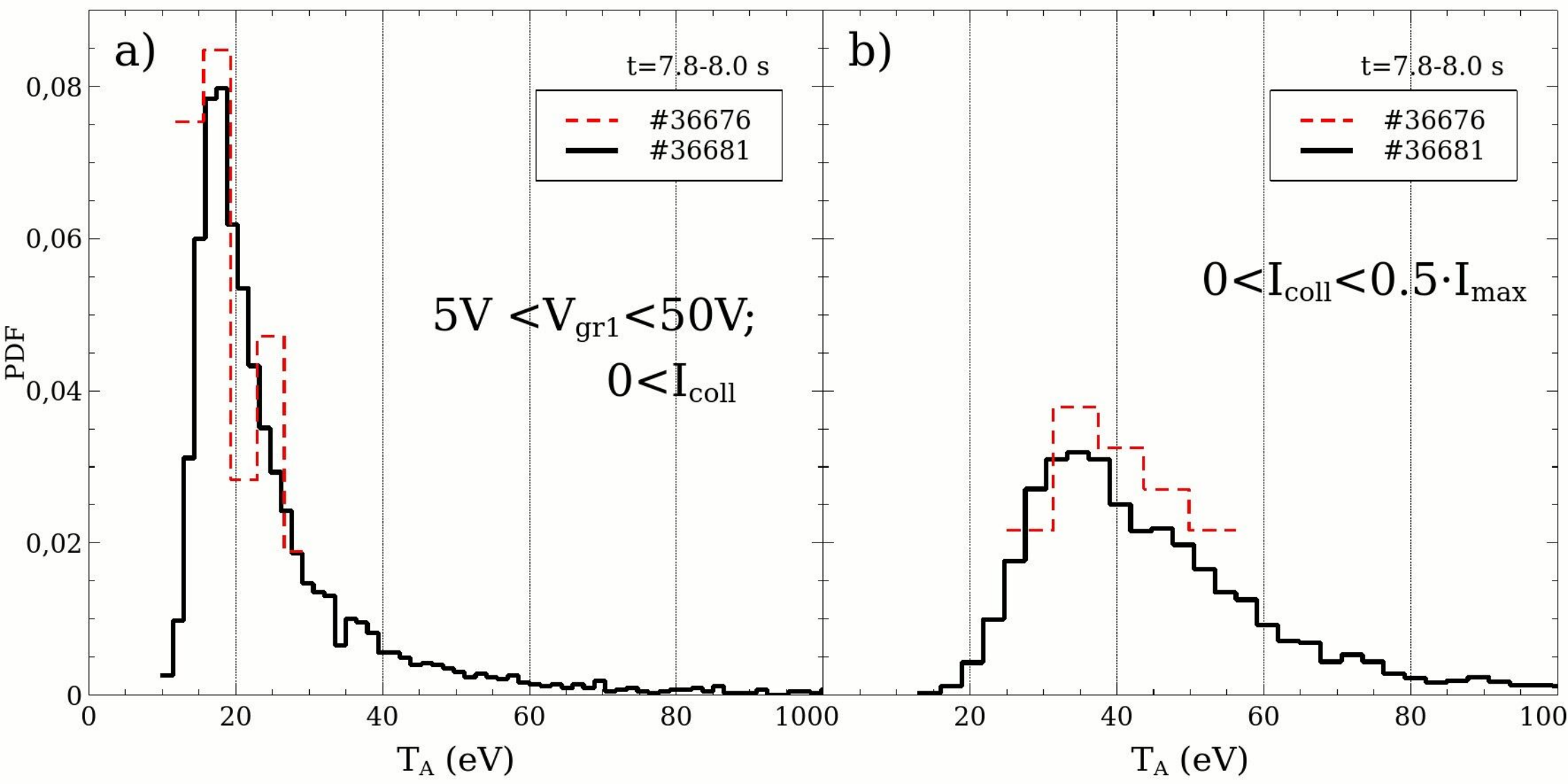
a)
t=7.8-8.0 s
#36676
#36681
5V <V$_{gr1}$<50V;
0<I$_{coll}$
PDF
0,08
0,06
0,04
0,02
0
0
20
40
60
80
1000
T$_A$ (eV)
b)
t=7.8-8.0 s
#36676
#36681
0<I$_{coll}$<0.5·I$_{max}$
20
40
60
80
100
T$_A$ (eV)

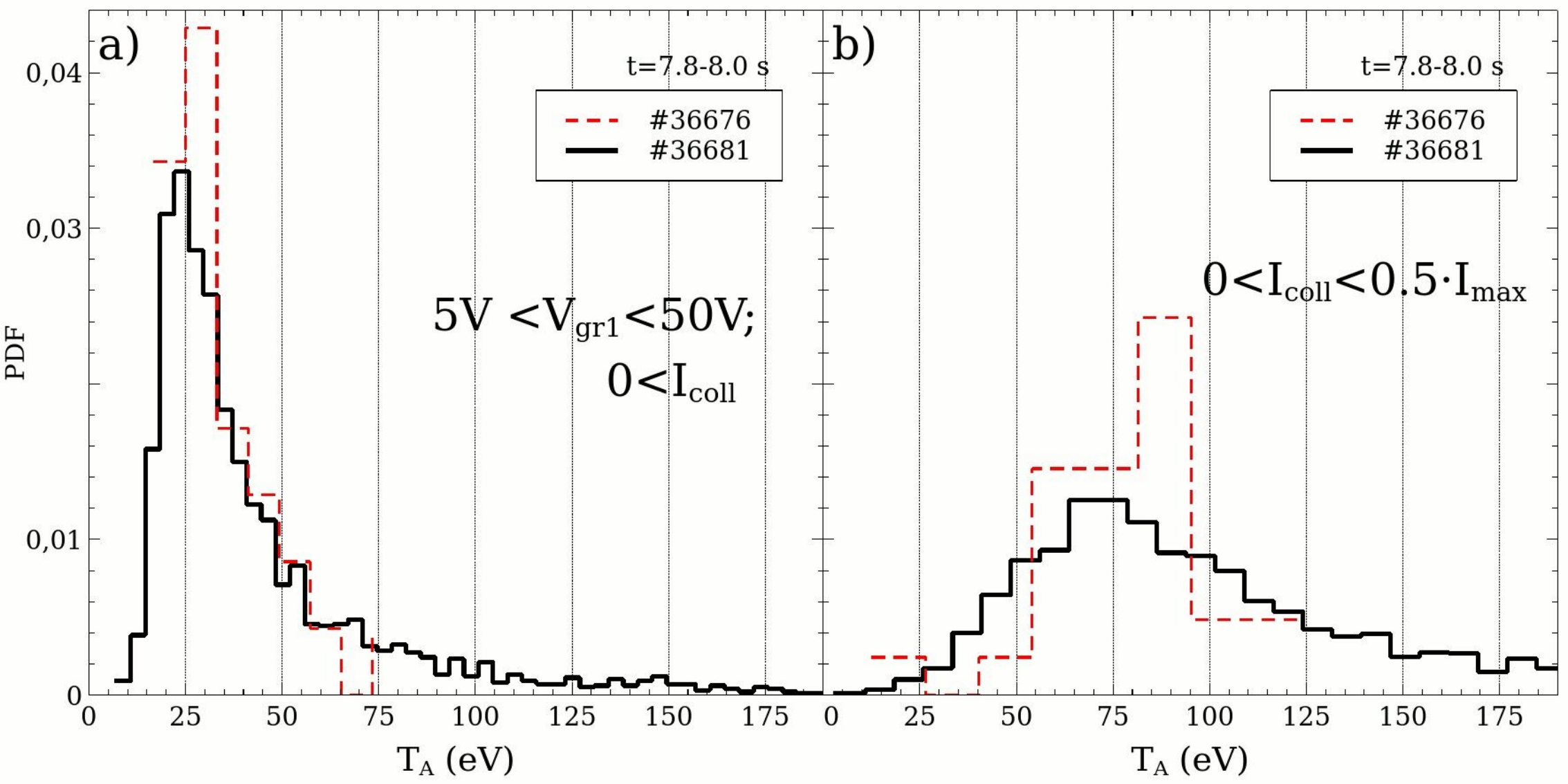
a)
t=7.8-8.0 s
#36676
#36681
5V <V$_{gr1}$<50V;
0<I$_{coll}$
PDF
0,04
0,03
0,01
0
0
25
50
75
100
125
150
175
T$_A$ (eV)
b)
t=7.8-8.0 s
#36676
#36681
0<I$_{coll}$<0.5·I$_{max}$
0
25
50
75
100
125
150
175
T$_A$ (eV)